

Results of the ROTOR-program

II. The long-term photometric variability of weak-line T Tauri stars ^{*}

K.N. Grankin¹, J. Bouvier², W. Herbst³, and S.Yu. Melnikov¹

¹ Astronomical Institute of the Uzbek Academy of Sciences, Tashkent, Uzbekistan, 700052

² Laboratoire d'Astrophysique, Observatoire de Grenoble, Université Joseph Fourier, B.P. 53, F-38041 Grenoble Cedex 9, France

³ Astronomy Department, Wesleyan University, Middletown, CT 06459

Received .../ Accepted ...

ABSTRACT

Context. T Tauri stars exhibit variability on all timescales, whose origin is still debated. On WTTS the variability is fairly simple and attributed to long-lived, ubiquitous cool spots.

Aims. We investigate the long term variability of WTTS, extending up to 20 years in some cases, characterize it statistically and discuss its implications for our understanding of these stars.

Methods. We have obtained a unique, homogeneous database of photometric measurements for WTTS extending up to 20 years. It contains more than 9 000 UBVR observations of 48 WTTS. All the data were collected at Mount Maidanak Observatory (Uzbekistan) and they constitute the longest homogeneous record of accurate WTTS photometry ever assembled.

Results. Definitive rotation periods for 35 of the 48 stars are obtained. Phased light curves over 5 to 20 seasons are now available for analysis. Light curve shapes, amplitudes and colour variations are obtained for this sample and various behaviors exhibited, discussed and interpreted.

Conclusions. Our main conclusion is that most WTTS have very stable long term variability with relatively small changes of amplitude or mean light level. The long term variability seen reflects modulation in the cold spot distributions. Photometric periods are stable over many years, and the phase of minimum light can be stable as well for several years. On the long term, spot properties do change in subtle ways, leading to secular variations in the shape and amplitudes of the light curves.

Key words. stars: rotation – stars: fundamental parameters – stars: starspots – stars: variables: general – stars: pre-main sequence – stars

1. Introduction

The third catalog of pre-main-sequence emission-line stars assembled by G. Herbig and collaborators includes 742 objects (Herbig & Bell 1988). Of these, about fifty objects were classified as weak-line T Tauri stars (WTTS). These include objects from X-ray surveys of several star-forming regions and from a survey of stars with CaII H and K emission lines. WTTS exhibit a weak, narrow $H\alpha$ line [$W(H\alpha) < 10\text{\AA}$], a strong LiI absorption line (6707 Å) with $W(\text{Li}) > 0.1\text{\AA}$, and a substantial CaII H and K emission lines.

The first photoelectric UBVR observations of these stars revealed periodic light variations in most WTTS (Rydgren & Vrba 1983; Rydgren et al. 1984; Bouvier et al. 1986, 1993, 1995; Grankin 1992, 1993, 1996; Vrba et al. 1993). Their photometric periods ranged from 1 to 10

days and were in agreement with spectroscopic estimates of their rotational velocities. It was assumed that the periodic light variations were due to the nonuniform distribution of cool photospheric spots over the stellar surface.

Rotation periods are now available for some hundreds of pre-main sequence and recently arrived main sequence stars of solar-like mass in five nearby young clusters: the Orion Nebula Cluster, NGC 2264, α Per, IC 2602 and the Pleiades (Mandel & Herbst 1991; Attridge & Herbst 1992; Eaton et al. 1995; Edwards et al. 1993; Choi & Herbst 1996; Bouvier et al. 1997a). In combination with estimates of stellar radii these data allow us to construct distributions of surface angular momentum per unit mass at three different epochs: nominally, 1, 2 and 50 Myr (see Herbst & Mundt 2005). Recent work is extending the age range to 200 Myr and adding many new clusters (Irwin et al. 2007).

The study of long-term variations in the main parameters of the light curves for young spotted stars is also of considerable interest. One would expect light-curve shapes

^{*} UBVR photometric data described in Table 1 are only available in electronic form at the CDS via anonymous ftp to cdsarc.u-strasbg.fr (130.79.128.5) or via <http://cdsweb.u-strasbg.fr/cgi-bin/qcat?J/A+A/>

to evolve as the spots change size, shape, temperature, or location, and a latitudinal migration of spots could cause changes in period, if the surfaces are in differential rotation, as in the Sun. It would, of course, be very interesting to find any cyclic pattern that could be interpreted as evidence for a magnetic cycle. Unfortunately, most of the photometric programs of observations of WTTS stars have been carried out episodically, in an interval from one to three months. Only one object (V410 Tau) has been investigated in detail over several seasons (Vrba et al. 1988; Herbst 1989; Petrov et al. 1994). These authors showed that there were at least two extended and long-lived spotted regions on the surface of V410 Tau during several years. The evolution of the shape and amplitude of the light curve from season to season was explained by changes in the spot sizes, temperatures, and relative locations.

The first systematic photoelectric BVR observations for about thirty WTTS in dark clouds in Taurus-Auriga began in 1990 at the Maidanak Observatory (Grankin et al. 1995). During 1990-1993 rotation periods were discovered for 12 WTTS and refined for another 9 WTTS. A fundamental result of the analysis of the photometric behavior of these WTTS was the stability of the initial epochs and rotation periods for 17 WTTS on a time scale from 2 to 4 years. In addition, there is a high detection rate of rotation periods among WTTS in the sample considered. It is generally believed that the stability of the initial epochs and rotation periods over several years indicates that the active region in each WTTS remains on a definite meridian over this time scale. Variations in the maximum brightness levels, the amplitudes and the shapes of the light curve for many WTTS is evidence for migration of the spots, within the limits of an active zone, and for changes in their size. It is interesting to note, that RS CVn and BY Dra stars show the same kind of long-term photometric behaviour and that active longitudes have long been reported on the Sun (Losh 1939). For RS CVn stars, active longitudes appear to persist for a number of years (Butler 1996). Thus, an activity mechanism with some similarities to that operating on the Sun may be indicated by these common observational characteristics with WTTS.

Longer term observations have shown, that the phenomenon of stability of the initial epochs is most pronounced in seven WTTS: LkCa 4, LkCa 7, V410 Tau, V819 Tau, V827 Tau, V830 Tau and V836 Tau (Grankin 1997, 1998, 1999). Changes in the phase of minimum light for these stars did not exceed $\pm 7\%$ of the period on a time scale from 7 to 12 years. Similar results were obtained for 23 WTTS in the young Orion Nebula Cluster (Choi & Herbst 1996).

Some interesting results have been received from analysis of long-term light curves of 30 WTTS and 80 RS CVn and FK Com stars (Grankin et al. 2002). These authors have found that in 18 of the 110 stars monitored, an increase in the amplitude of the periodic variability accompanies a rise of the maximum brightness level. This result is difficult to understand in the context of a simple model

where the star contains only a single spotted region in a high latitude zone that is always visible, because increasing the size of the spot (as required to increase the amplitude) should decrease the maximum brightness of the star. It is possible to explain such behavior by invoking a star covered with multiple spots at different latitudes. In this case the amplitude will not depend just on the total area of the spots, but will also depend on the distribution of these spots on the stellar surface. Similar results have been obtained recently for 24 WTTS stars in the extremely young cluster IC 348 over five observing seasons (Cohen et al. 2004). It has been shown that the stability of average magnitude from season to season most likely indicates that spots on these WTTS stars tend to redistribute themselves and undergo changes in size, temperature, and location rather than simply appear or disappear *en masse*.

The observations to date support to the possible existence of stellar activity cycles on WTTS. In an attempt to find and study such activity cycles we have continued to monitor some tens of WTTS at Mt. Maidanak Observatory over many years. In this paper, we employ the unique and extensive Mt. Maidanak database to investigate WTTS variability on a time scale of many years and, in some cases, multiple decades. In Section 2, we describe the stellar sample and the observations carried out for the last 20 years at Mt. Maidanak. In Section 3, we discuss the phenomenon of rotational modulation of the light curves of 36 WTTS. In Section 4, we describe a spot model and some results of modeling. In Section 5, we define the statistical parameters used to characterize the long term variability of WTTS. Further modeling of the light curves will be presented in a later paper in this series.

2. Star sample and observations

All *UBVR* data were obtained at Mount Maidanak Observatory (longitude: $E4^h27^m47^s$; latitude: $+38^\circ41'$; altitude: 2709 m) in Uzbekistan. Results of astroclimate studies at Maidanak observatory have been summarized by Ehgamberdiev et al. (2000), who show that it is among the best observatories in the world, in many respects. We targetted 48 WTTS for long-term monitoring, mostly from the list of Herbig & Bell (1988). More than 9000 *UBVR* magnitudes were collected for these objects between 1990 and 2004, although the number of U magnitudes is relatively small compared to the other colors due to the faintness of the stars at those wavelengths. All the observations were obtained at three telescopes (two 0.6 and one 0.48 m reflectors) using a single-channel pulse-counting photometer with photomultiplier tubes. As a rule, each program star was measured once per night at minimal airmass. We secured between 12 and 30 (*U*)*BVR* measurements for each sample target during each observational season lasting several months. The number of measurements depends on the object's visibility from Mt. Maidanak. The largest number of measurements was thus obtained for WTTS in Taurus, and fewer in Ophiuchus and Orion. Magnitudes are provided in the Johnson *UBVR* system. The rms error

of a single measurement in the instrumental system for a star brighter than 12^m in V is about $0^m.01$ in BVR and $0^m.05$ in U .

Observations were carried out either differentially using a nearby reference star (see Strauzis 1977) or directly by estimating the nightly extinction (Nikonov 1976). In the latter case, several reference stars were observed every night to derive the extinction coefficients in each filter. Selected standard stars (Landolt 1983, 1992) were observed and used to transform instrumental magnitudes into the Johnson/Cousins $UBVR$ system. We then transformed the magnitudes to the Johnson $UBVR$ system using the relationship from Landolt (1983) : $(V-R)_C = -0.0320 + 0.71652 \times (V-R)_J$. The formal accuracy of this reduction step is $0^m.01$. All observed local times have been converted to heliocentric julian days (JDH). A detailed description of the equipment, observation techniques, and data processing is given in Shevchenko (1989).

Results of the Mt. Maidanak program of homogeneous, long-term photometry of WTTS are summarized in Table 1. Columns are: star's name, star's number in the Herbig & Bell (1988) catalogue, spectral type, time span of observations in JD, number of seasons observed, photometric range in the V band, number of observations in the V band, and average values of $B - V$ and $V - R$ colors. In the last column we give a multiplicity indicator, as follows: spectroscopic binary (SB), visual binary (VB), and visual tertiary (VT). The complete Maidanak database for WTTS is available in electronic form at CDS, Strasbourg, via anonymous ftp to cdsarc.u-strasbg.fr.

Most of the objects are located in the Taurus-Auriga region (40 of the 48) and only 8 WTTS are in other star forming regions. The range of spectral types is from G0 to M4. There are eight stars in the range G0 to G9, eighteen between K0 and K5, ten between K6 and K9, and nine between M0 and M4.

3. Results of periodogram analysis

The light curves obtained during the ROTOR campaign were analyzed using the PERIOD software time-series analysis package (see Starlink User Note). Periods were searched for each season using two different methods, a chi-squared technique and the Lomb-Scargle periodogram analysis. The first method is straight-forward and the input data are simply folded on a series of trial periods. At each trial period, the data are fitted with a sine curve. The resulting reduced- χ^2 values are plotted as a function of trial frequency and the minima in the plot suggest the most likely periods. See Horne et al. (1986) for an example of the use of this method, which is ideally suited to the study any sinusoidal variations. The second method is a novel type of periodogram analysis, quite powerful for finding, and testing the significance of, weak periodic signals in unevenly sampled data (see Horne & Baliunas 1986; Press & Rybicki 1989). As both methods have shown very similar results, here we simply adopt the periods de-

termined by the commonly used Lomb-Scargle method and these are reported in Table 2.

False-alarm probabilities (FAP1) for the period were computed using a Fisher randomization test, or Monte-Carlo method (see, for example, Nemeč & Nemeč 1985). FAP1 represents the proportion of permutations (ie. shuffled time-series) that contained a trough lower than (in the case of the chi-squared method) or a peak higher than (in the case of the Lomb-Scargle periodogram analysis) that of the periodogram of the unrandomized dataset at any frequency. This therefore represents the probability that, given the frequency search parameters, no periodic component is present in the data with this period. To ensure reliable significance values, the minimum number of permutations was set to 1000. If the false alarm probabilities lie between 0.00 and 0.01, then the quoted period is a correct one with 95% confidence. Periods were searched for within an interval ranging from 1 day to 20 days. The periodogram is computed at 1000 frequencies between 0 and 0.05 d^{-1} .

A search for a periodic component has been made for all stars in Table 1. Results of the periodogram analysis are listed in Table 2 for the 36 stars which showed a significant periodicity in one season of observation or more. No significant periodicity was found for the other 12 stars. We give the values of periods for which the FAP1 lies between 0.00 and 0.01. If the false alarm probabilities lies between 0.01 and 0.05, the period is designated by a sign ":". If the FAP1 lies between 0.05 and 0.10, the period is designated by a sign "?:". Absence of any periodicity is designated by a sign "-". In last column the most significant period, based on a periodogram for the entire observing interval (i.e. for all seasons) is presented.

We have tried to improve the period and ephemeris for each star in Table 2 by the following procedure. Each seasonal lightcurve was folded with its mean period to determine the time of minimum T_0 by fitting a polynomial to the folded lightcurve. We used the value for the period given in the last column of the Table 2 to compute the number of cycles elapsed between each of the seasonal points T_0 and the time of minimum observed by us. Then we computed the O-C diagram for the minima T_0 as a function of cycle number. The residuals in this diagram can be minimized by modifying the period. In this way a best fit period and new ephemeris for each star are found. See Stelzer et al. (2003) for an example of the use of this method for updating of the period and ephemeris for V410 Tau. The new period and ephemeris for each star are given in Table 3. We adopt this ephemeris and period for all further analysis.

4. Rotation modulation phenomena

Thirty-six of our 48 WTTS exhibit periodic light variations during one or more seasons. A list of these objects is given in Table 3. Columns are: star's name, the epoch of our observations, the minimum and maximum amplitudes of the periodic light variations (ΔV_{min} and ΔV_{max}), the

initial epoch, the rotational period, and two columns of references. The first column with references contains the papers in which there is a first mention of a period. The second column with references specifies the papers from which we have taken the initial epoch and the more precise value for a period.

Minimum amplitudes of the periodic light variations are in the range of $0^m.05$ to $0^m.4$ in the V band (see Figure 1) but more than 80% of stars have minimum amplitudes in the interval from $0^m.05$ up to $0^m.1$. Maximum amplitudes of the periodic light variations range from $0^m.15$ to $0^m.8$ in V and 75% of the stars show a maximum amplitude within the limits of $0^m.15$ to $0^m.3$. The peak of this distribution is at $0^m.15$. The stars with the highest amplitudes of periodic light variations, achieving $0^m.4 - 0^m.8$ in the V band, are: LkCa 4 ($0^m.79$), V410 Tau ($0^m.63$), V836 Tau ($0^m.62$), LkCa 7 ($0^m.58$), V827 Tau ($0^m.51$), and V830 Tau ($0^m.45$). Such large amplitudes of the light variation indicate the existence of very extended spotted regions on the stellar surface. Note that some stars were observed at fewer epochs than others, so we cannot be sure that the quoted values of ΔV_{min} and ΔV_{max} , especially in these cases, are truly representative of the stars behavior on a time scale of decades. The actual extrema in these values may be larger than is represented on Figure 1.

Of the 36 targets with periods, 35 lie within the range 0.48 to 9.9 days (see Table 3). The star TAP 4 shows the shortest period, $P = 0.482$ d, and TAP 45 shows the longest period of these 35, with $P = 9.9$ d. The most common periods are within the interval 0.5 to 4 d (see Figure 2). The exceptional star is V501 Aur. Its photometric period is close to 56 days, and it is most likely not a rotation period. We may estimate the luminosity and radius of this star, assuming, that it is associated with the Taurus dark clouds at a distance of 140 pc. In that case, if the photometric period corresponds to the period of rotation, its equatorial speed of rotation would be about 3 km/s, which contradicts its measured value of 25-27 km/s. It is possible that this object belongs to another class of variable stars; spectral observations are required to confirm or deny this guess.

Perhaps the most interesting result from our long-term observations is that the phase light curve (φ_{min}) may be conserved for times as long as several years. This phenomenon of stability is most pronounced in V410 Tau (see Figure 3). Over 19 years of observation, the changes of φ_{min} have not exceeded 0.16 P, where P is the rotation period (Stelzer et al. 2003). We can see another example of phase stability extending for 15 years in LkCa 7 (Figure 4). Out of the total sample, 7 stars show such stability of φ_{min} for time intervals between 5 and 19 years, namely: LkCa 4, LkCa 7, V410 Tau, V819 Tau, V827 Tau, V830 Tau, and V836 Tau. Such long-term stability of φ_{min} is probably due to the existence of so-called active longitudes at which the (shorter-lived) extended spotted regions are located (Grankin et al. 1995). Such active longitudes have been reported on the Sun and RS CVn stars. It should

be noted, that the majority of these stars (6 of 7) also are among the stars with the highest photometric amplitudes, i.e. they are the most active variable stars in our sample. We suppose, that the phenomenon of stability of φ_{min} is connected somehow with level of activity.

All the stars in our sample show significant changes in amplitude and shape of phased light curves from season to season without any dependence on their stability or instability of minimum phase. For example, in the case of V410 Tau, the amplitude changes from $0^m.39$ till $0^m.63$. In the case of LkCa 7 the amplitude changes from $0^m.33$ to $0^m.58$. It is worth noting that the most symmetric phased light curve around φ_{min} generally corresponds to the season with the maximum amplitude. On the other hand, the most asymmetrical phased light curves typically correspond to seasons with the minimum amplitudes of light variability (see Figure 3-4). We note that one object in our sample showed a very unusual shape for a phased light curve in some seasons. This is LkCa 4, which in 1992, 1993, and 1995 displayed a flat portion near minimum in the phased light curve (see Figure 5). All other stars show constantly changing, in many cases nearly sinusoidal light curves as a rule. In addition, this star has shown the record amplitude in 2004, of about $0^m.8$ in the V band. We do not know of another star of any type with such a large amplitude caused by the phenomenon of rotational modulation.

While some stars (such as V410 Tau, LkCa 7, and LkCa 4) show gradual changes of amplitude and shape from season to season, there are examples of other behaviour. The amplitude of the periodic light variations may appreciably change by as much as a few tenths of a magnitude from one season to the next, as in case of TAP 41. We can see from Figure 6 that the phased light curve remains stable for two seasons, 1992 and 1993, after which its initial phase and shape evolve rapidly. During such periods of rapid light curve evolution, it is often not possible to detect the star as a periodic variable or, if detected, its amplitude is quite small, as in 1994 and 1998.

It may be noted, that for the majority of stars the average level of light does not change even as the amplitude decreases considerably. TAP 41 nicely illustrates this. It has been shown that the stability of average level of light from season to season most likely indicates that spots on WTTS tend to redistribute themselves and undergo changes in size, temperature, and location rather than to appear or disappear *en masse*. However, it is also necessary to note, that some stars do show significant changes in their average level of light from season to season. Examples are: TAP 50, V819 Tau, V827 Tau, V836 Tau, and VY Tau.

There is one more example of unusual photometric behaviour among our sample of WTTS. It may be seen on Figure 7 that the amplitude of the light curve of V830 Tau changed by a few tenths of a magnitude from its normal value during the 2002 and 2003 seasons. During this period of time the phase light curve also had a complex shape in the sense that two maxima and two minima were observed per cycle. Such shapes of light curves can be the

result of the existence of two extended spotted regions on opposite sides of the star. Similar light curves were observed at two epochs for V410 Tau in 1981/1982 and in 1983/1984 (see Herbst 1989).

Preliminary analysis of our long-term observations revealed an interesting relation between the variation of the amplitude of the variability and the change in the level of maximum brightness between different seasons. We noticed that some WTTS show an increase of the amplitude of their variability accompanied with the rise of the maximum level of brightness. The maximum brightness as a function of the amplitude of the light curve for 4 such WTTS are shown in Figure 8. The increase of the amplitude with the maximum level of brightness is clearly visible on this Figure. This result is difficult to explain in a model of a star spotted with a single, high latitude spot. Increasing the area of such an almost-polar spot would decrease the maximum brightness while increasing the amplitude of the light curve, which is opposite to our measurements. A model with two nearly-polar spots in opposite hemispheres can explain the observations if the inclination angle of the star is sufficiently large so that both spots contribute to the light variations. In this case, it would be the motions of the spots in longitude that would account for the amplitude variation, not the growth or decay of a spot (see Grankin et al. 2002).

In this connection we have investigated how V_{min} , V_{max} and V_{mean} change with amplitude. We found four groups of stars with different dependences between V_{min} , V_{max} , V_{mean} and amplitude. The first group of stars includes V410 Tau, LkCa 1, LkCa2, LkCa 7, TAP 26, TAP57, and SR 9. In all these cases, when the amplitude increases, V_{max} decreases (i.e. the star brightens), while V_{min} increases, and the mean light level remains about constant. In Figure 9, the long term variations of V_{min} , V_{max} and V_{mean} as a function of V amplitude for V410 Tau are presented. We can see that V_{max} increases, and V_{min} decreases when the amplitude increases. However, as the lower right panel of the figure shows, there is no correlation between V_{max} and V_{min} .

A second group of stars exists which does show real dependence between V_{max} and V_{min} (they decrease or increase simultaneously). These stars are: LkCa 19, TAP 35, TAP 40, TAP 50, V819 Tau, V836 Tau, V1200 Tau and V1202 Tau. It may be noted, that these stars do not show any reliable dependence between amplitude, V_{max} and V_{min} . A third group of stars shows dependence between amplitude and V_{min} , but does not show dependence between V_{max} , V_{mean} and amplitude. These are: Anon1, HD283572, LkCa 3, LkCa 4, Wa Oph/2, Wa Oph/3, V827 Tau, and SR 12. A fourth group does not show any dependences. These stars are: LkCa 11, V1197 Tau, V1207 Tau, Wa Oph/1, VY Tau. In addition there are 3 stars which we cannot classify unequivocally as belonging to any of these groups, namely TAP 45, V830 Tau, V1199 Tau.

To summarize, all of the stars in Table 3 exhibit the phenomenon of rotational modulation. But evolution of phased light curves occurs in a variety of man-

ners. Some show specific dependencies between amplitude, V_{min} , V_{max} and V_{mean} , but these are in various directions and some stars show no such dependencies. Detailed modeling of these behaviors is beyond the scope of the present paper and will be presented elsewhere. However, here we have used a simple model of the spots to analyze some features of the light curves and suggest reasons for the phenomena exhibited above.

5. Preliminary Spot model and Some Results

Models of light curves of TTs have been made based on assumed geometries of the spots, e.g. one or two circular spots (Bouvier & Bertout 1989; Herbst 1989), while other models have used only certain properties of the light variations such as amplitude as a function of wavelength to infer a spotted regions (SR) general parameters, without assumptions about its geometry (Bouvier et al. 1993). Assessment of advantages and disadvantages of particular models is beyond the scope of our study and it is certainly a good idea to model the data in a variety of ways. Here we simply note that the non-uniqueness of light curve solutions means that the choice of particular geometries for the spots needs to be motivated by something other than the light curve data themselves. For instance, Alekseev & Gershberg (1996a) justifiably criticize attempts to use parametric models to study the surface nonuniformity of red dwarf stars with solar-type activity. Such models normally assume the existence of two high-latitude spots near the stars magnetic poles, while long-term photometric observations of red dwarfs provide evidence for the existence of low-latitude spotted zones. Accordingly, Alekseev & Gershberg (1996b) propose a model of zonal spottedness for these stars, in which a collection of starspots is approximated by two symmetric (about the equator) dark strips with a variable spot-filling ratio in longitude. For WTTS, the situation with the choice of a particular spottedness model is not yet so certain.

On the one hand, the first detailed Doppler images of the surfaces of the two brightest WTTS (V410 Tau and HDE 283572), which were obtained by analyzing variations in the line profiles over the rotation period, suggested that there were large cool spots at high latitudes (Joncour et al. 1994a,b). The origin of such high-latitude spots can be explained by the existence of a dipole magnetic field, whose presence is assumed by some current models that describe the interaction between a young star and a disk (see for example Shu et al. 1994). On the other hand, we discussed above that, based on the photometry of 36 periodic WTTS, there is a similarity in behavior with main-sequence dwarfs, BY Dra stars, and with RS CVn stars. So, it is arguable that some similarities exist to solar-type activity. In this case, the long-term evolution of the photometric light curves for WTTS may be improperly explained in terms of a model with only one or two large, high-latitude spots.

Here we will assume that there are many spots or groups of spots on the surfaces of WTTS, including at

high latitude. Analysis of the Doppler images of the surface of V410 Tau obtained by Rice & Strassmeier (1996) provides evidence for the existence of both high-latitude and low-latitude spots, consistent with this assumption. We believe that the number of spots and their distribution over the WTTS surface remains an open question. Accordingly, for our quantitative analysis of the spottedness parameters for the WTTS, we used a model whose parameters do not depend on the number, shape, and positions of the spots. This non-parametric model allows only the total area and mean temperature of the spots in the visible stellar hemisphere to be estimated. A detailed description of this model can be found in Bouvier et al. (1993); Grankin (1998, 1999).

Vogt (1981) showed that the light variations of a star due to the spottedness of its photosphere can be written as

$$\Delta m(\lambda) = -2.5 \log \left\{ \frac{1 - [1 - S(\lambda)]G_{max}(\lambda)}{1 - [1 - S(\lambda)]G_{min}(\lambda)} \right\}, \quad (1)$$

where $S(\lambda)$ is the ratio of the surface brightness of the SR to the brightness of the photosphere; and $G_{max}(\lambda)$ and $G_{min}(\lambda)$ are the spot areas at maximum and minimum SR visibility, respectively. The spot area depends on the wavelength via the limb-darkening coefficient of the star. If we know the absolute maximum brightness of the star, when its visible hemisphere is completely free from spots ($G_{min} = 0$), then equation (1) for the time of maximum SR visibility can be written as

$$m_{min}(\lambda) - m_{max}^{abs}(\lambda) = -2.5 \log \{1 - [1 - S(\lambda)]G_{max}(\lambda)\}, \quad (2)$$

where $m_{max}^{abs}(\lambda)$ is the star's absolute maximum brightness, and $m_{min}(\lambda)$ is its minimum brightness in a specific observing season.

If the limb-darkening effect is ignored, then the spot area can be assumed to be independent of wavelength. In the case of a broadband photometric system, relation (2) for V then takes the form

$$V_{min} - V_{max}^{abs} = -2.5 \log \{1 - [1 - L_V]G_{max}\}, \quad (3)$$

where $L_V = (\int I_{sp}(\lambda)\Phi_V(\lambda)d\lambda) / (\int I_{ph}(\lambda)\Phi_V(\lambda)d\lambda)$, $I_{ph}(\lambda)$ and $I_{sp}(\lambda)$ - are the energy distributions in the photosphere and the SR, respectively; $\Phi_V(\lambda)$ - is the response curve of the V filter; V_{min} is the minimum V brightness for a specific observing season; and V_{max}^{abs} is the absolute maximum V brightness of the star. Equation (3) contains two free parameters - the integral of the energy distribution for the SR, which is uniquely related to the SR effective temperature, and the spot area at maximum SR visibility. These two free parameters can be determined by solving the system of two equations of type (3) written for the V and R bands.

It may be noted that results of the computer simulation strongly depend on the assumed spot-free bright-

ness of the star. Many authors assume that the observed maximum brightness of the star (V_{max}) corresponds to a spot-free configuration. In this case, however, the phased light curve may be expected to have a plateau at maximum light., something that is rarely or never seen. Also, in this case a star's maximum brightness could not depend on the amplitude of variations, as found for some stars. It may be seen on Fig. 8 that a decrease in periodicity amplitude is accompanied by a decrease in the star's maximum brightness in these cases. This demonstrates that, for these stars, the brighter stellar hemisphere is not completely free from spots. The stellar photospheres of all TTs most likely remain spotted to some degree at all phases of axial rotation. Thus, the observed maximum brightness of a star is not the absolute maximum brightness of a spotted star. It is quite clear, therefore, that only lower limits on the parameters of spotted regions can be determined by using the observed maximum brightness of the star as (V_{max}^{abs}) (see also the discussion in Bouvier et al. 1993).

We attempted to obtain more realistic estimates of the SR parameters by using a linear relation between the amplitudes of the periodicity in V and R. At minimum spot visibility, V_{max}^{abs} is related to V_{max} by

$$V_{max} - V_{max}^{abs} = -2.5 \log \{1 - [1 - L_V]G_{min}\}. \quad (4)$$

We see from (4) that for V_{max}^{abs} to be determined, we must know the degree of spottedness of the stellar surface at minimum spot visibility. The following system of equations can be used to estimate G_{min} :

$$\begin{cases} V_A = -2.5 \log \left(\frac{1 - [1 - L_V]G_{max}}{1 - [1 - L_V]G_{min}} \right) \\ R_A = -2.5 \log \left(\frac{1 - [1 - L_R]G_{max}}{1 - [1 - L_R]G_{min}} \right), \end{cases} \quad (5)$$

where V_A and R_A are the amplitudes of the periodicity in V and R, respectively. We derived the equation for V_A by subtracting equation (4) from (3). The equation for R_A was derived in a similar way.

From the set of G_{min} values obtained by solving (5), we choose only those which satisfy the relation

$$V_{max}^{abs} - R_{max}^{abs} \cong (V - R)_o, \quad (6)$$

where $(V - R)_o$ is the normal color index of the star that corresponds to its spectral type; V_{max}^{abs} and R_{max}^{abs} are the maximum V and R brightness of the star estimated by substituting G_{min} into equation (4) written for the V and R bands, respectively.

In other words, the star's $V_{max}^{abs} - R_{max}^{abs}$ color index corrected for the reddening due to the spottedness of the stellar surface must essentially match its normal color index. In this case, we obtain an upper limit on V_{max}^{abs} , which obviously differs from the observed value V_{max} . The SR parameters determined from the upper limit on V_{max}^{abs} are overestimated compared to their values calculated by assuming that $V_{max}^{abs} = V_{max}$. For this reason, we call the

SR parameters calculated by the above method the upper limits on the spottedness parameters.

With the goal of testing of our model we have estimated the spottedness parameters for VY Ari and compared our results with the results that were obtained by Alekseev & Gershberg (1996a,b) by using their model of zonal spottedness. The testing shows that the two models yield similar results, despite the significant differences between the two algorithms. For example, the difference in the estimated effective spot temperatures (ΔT) is 100 K, while the difference in the estimated fractional spot areas ($\Delta G/G$) does not exceed 2.5-3.5%. All these facts suggest that, despite its simplicity, our model allows the main spot parameters to be estimated with a sufficient accuracy (see Grankin 1998).

For the stars with the highest light curve amplitudes, this model shows that the spotted regions cover from 17 to 73% of the visible stellar hemisphere and that the mean temperature of the spots is 500-1400 K lower than the ambient photosphere. An analysis of the calculated spot parameters of V410 Tau revealed that there is a real correlation between the amplitude of periodicity (ΔV) and the spot distribution nonuniformity (ΔG), which is defined as the difference of spot coverage in the visible hemispheres of the star at maximum and minimum light: $\Delta G = (G_{max} - G_{min}) * 100\%$, and G_{max} and G_{min} are the area of the spotted region at maximum and minimum spot visibility, respectively. As the amplitude increases from $0^m.39$ to $0^m.63$, the degree of nonuniformity in the spot distribution increases from 21 to 37%. By contrast, the amplitude is essentially independent of the variations in total spot area S , where $S = 0.5 * (G_{max} + G_{min}) * 100\%$. Therefore, the change in the amplitude has to be caused by a change in the distribution of the star spots rather than by a change in the total spot area. This is shown in Fig. 10 on the upper panel, where we plot the amplitude versus the degree of non-uniformity in the spot distribution (ΔG) and versus the total spot area (S).

Besides, the computer simulation has shown that the average magnitude (\bar{V}) depends on the total spot area (S) and it does not depend almost on the degree of non-uniformity in the spot distribution (ΔG). As the average magnitude decreases from $10^m.80$ to $10^m.95$, the total spot area increases from 44 to 53% (see Fig. 10, inferior panel). Thus, the cycles of star activity should be exhibited in quasi-cyclic variations of the average magnitude from season to season. Some WTTS from our sample may demonstrate such quasi-cyclic variations of the average magnitude. We are going to continue our photometric monitoring of selected spotted stars in an effort to detect and study the cycles of stellar-activity.

6. The long term variability of WTTS

In Paper I we have undertaken a statistical analysis of the long-term light curves of classical T Tauri stars (CTTs) (Grankin et al. 2007). We have presented and characterized the long term photometric variations of 49 CTTs over

as much as 20 years and proposed an empirical classification scheme. We here apply the same statistical analysis to the long term variability of WTTS.

As in Paper I, we first define a set of statistical parameters which allow us to characterize the long term photometric variability of WTTS. In order to get robust statistical estimates, we consider only the 33 stars that have at least 5 observing seasons containing at least 12 photometric measurements per season. As shown in Paper I, this selection provides reliable statistical estimates of their variability. For each object, we compute the mean light level ($V_m^{(i)}$) in each season (i) and the corresponding photometric range ($\Delta V^{(i)}$). The mean of ($V_m^{(i)}$) over all seasons yields the mean light level of the object (\bar{V}_m) while its standard deviation (σ_{V_m}) measures the scatter of the seasonal means. Similarly, we compute the average V band photometric amplitude over all seasons ($\overline{\Delta V} = \frac{\sum \Delta V^{(i)}}{N_s}$, where N_s – number of observational seasons) and its standard deviation ($\sigma_{\Delta V}$). We also make use of the ratio $\frac{\sigma_{\Delta V}}{\overline{\Delta V}}$. Two additional parameters were defined in Paper I, namely $C1 = \langle \frac{V_{med} - V_{min}}{\Delta V} \rangle$, where V_{med} is the median light level of the object in a given season, V_{min} its maximum brightness level and ΔV its photometric amplitude during this season and the bracket indicates an average over all seasons, which measures the preferred brightness state of the object, and $C2 = \sigma_{V_{min}} / \sigma_{V_{max}}$, which characterizes the relative seasonal variability of the maximum and minimum light levels.

In addition to the statistical parameters above, we also characterize the long term photometric behaviour of WTTS by investigating their colour variations. Previous studies of the short term variability of WTTS have shown that most stars tend to redden in colour indices (such as $V - R$) when fading (e.g. Herbst et al. 1994). This behavior can result from surface cold spots (cf. Bouvier et al. 2005). Some illustrations of the linear relations found for most objects between the $V - R$ colour and V magnitude are given on Fig. 11. We characterize the colour behaviour of WTTS by computing the color slopes $\frac{\Delta(B-V)}{\Delta V}$ and $\frac{\Delta(V-R)}{\Delta V}$ from least-square fits, and the correlation coefficients ρ_{B-V} and ρ_{V-R} . We used the full set of data pertaining to each object in order to compute these parameters.

The resulting values of the statistical and colour parameters for 33 WTTS whose light curves are shown in Fig.12a and 12b are listed in Table 4. The columns in Table 4 provide the star's name, the number of seasons N_s^* with at least 12 measurements, the mean brightness level (\bar{V}_m) and its seasonal standard deviation (σ_{V_m}), the average photometric range ($\overline{\Delta V}$, averaged over all seasons) and its seasonal standard deviation ($\sigma_{\Delta V}$), the fractional variation of photometric amplitude as measured by the ratio $\frac{\sigma_{\Delta V}}{\overline{\Delta V}}$, the color slope $\frac{\Delta(B-V)}{\Delta V}$, their correlation coefficient ρ_{B-V} , the color slope $\frac{\Delta(V-R)}{\Delta V}$ together with their correlation coefficient ρ_{V-R} , and the parameters C1 and C2.

6.1. General photometric properties

WTTS usually exhibit a low level of variability. A histogram of the average V-band amplitude for the 33 WTTS in our sample is shown in Fig. 13. The distribution is quite peaked, with $\overline{\Delta V}$ ranging from $0^m.1$ to $0^m.55$. Indeed, 28 WTTS (85%) in our sample exhibit small ranges of variability between $0^m.1$ and $0^m.3$, and only 5 (15%) have average V-band amplitudes larger than $0^m.4$ (LkCa 4, LkCa 7, SR 9, V410 Tau, and V836 Tau). The mean light level of WTTS also appears very stable over the years, with an exceedingly small standard deviation σ_{V_m} . Its distribution is shown by the histogram in Fig. 14, with the vast majority of WTTS having $\sigma_{V_m} \leq 0^m.05$. Only one object, V836 Tau, exhibits significant changes in average brightness over the years, with $\sigma_{V_m} = 0^m.2$. Similarly, the variations of photometric amplitude from season to season are small, amounting to less than $0^m.1$ for most WTTS, as shown by the histogram of $\sigma_{\Delta V}$ in Fig. 15.

WTTS also exhibit a fairly straightforward $V - R$ colour behaviour, turning redder when fainter. For most objects in our sample, the $(V - R)$ index scales linearly with brightness, with a correlation coefficient higher than 0.47 for 26 WTTS. An illustration is provided in Fig. 11. Only 7 stars do not show any reliable dependence of $V - R$ on brightness (correlation factor of lower than 0.47) when averaged over all seasons. These stars are: SR 12, TAP 35, V501 Aur, V1197 Tau, V1207 Tau, Wa Oph/2, and Wa Oph/3. The linear relation is replaced by a wide scatter of points on the diagram for these stars.

A histogram of $\frac{\Delta(V-R)}{\Delta V}$ color slopes for the 26 WTTS with linear color variations is shown in Fig. 16. It strongly peaks at values of 0.2–0.4. In WTTS, brightness and color variations result from the rotational modulation of the stellar flux by cold surface spots. We showed in Paper I that CTTS exhibit the same average $\frac{\Delta(V-R)}{\Delta V}$ color slope as WTTS. This might be an indication that the photometric variability of CTTS is also dominated by cold spots, but hot spots as well as circumstellar extinction can produce this kind of $V - R$ color variations as well (Bouvier & Bertout 1989).

A similar analysis was carried out for the $B - V$ index. Unlike the $V - R$ index, $B - V$ variations show little correlation with brightness, as seen from the low value of the correlation coefficients listed in Table 4. Only 3 stars (TAP50, V410 Tau, and V827 Tau) show a reliable dependence of $B - V$ on brightness (correlation factor larger than 0.47) when averaged over all seasons. The lack of a correlation between brightness and B-V colour could be due to flares and/or chromospheric variability.

6.2. Correlated properties

In Paper I, we investigated the relationships between the various statistical parameters we defined for CTTS. We do the same here for WTTS and contrast the results with those obtained for CTTS.

Fig. 17 and 18 show plots of the statistical parameters against each other that had allowed us in Paper I to identify various photometric subgroups within the CTTS sample, corresponding to specific sources of variability (cold spots, hot spots, circumstellar extinction). In contrast, WTTS appear in all these plots as an homogeneous photometric group characterized by a low level of variability as compared to CTTS. This confirms that the photometric variability of WTTS is dominated by a single process, namely the rotational modulation of the stellar flux by cold surface spots. In other words, the usually very stable long term (years) photometric variability of WTTS merely reflects spot modulation on much shorter timescales (weeks). Although we do not find any clear correlation in WTTS between the various variability proxies, the same trends found for CTTS over a much larger photometric range are seen, such as, e.g., a correlated increase of average amplitude and its seasonal variations (Fig.17).

The more complicated $C1$ and $C2$ parameters proved useful to distinguish the various sources of photometric variability in CTTS (see Paper I). WTTS are shown in the same plot in Fig. 18. Except for one peculiar WTTS, V830 Tau, all WTTS scatter around the mean value of these 2 parameters. This indicates that they have no preferred brightness state ($C2$), and that their extreme brightness levels ($C1$), high and low, vary by about the same amount (see, e.g., LkCa7, V410 Tau, TAP 50 in Fig. 11b). The isolation of V830 Tau on this diagram occurs because $\sigma_{V_{max}}$ is three times greater than $\sigma_{V_{min}}$. No WTTS are found in the lower left corner or in the upper right corner of this plot, which were shown in Paper I to correspond to UXor-type circumstellar extinction events and hot spot dominated variability, respectively. This is again consistent with the cold surface spots being the dominant and probably single source of variability in WTTS.

Conversely, we note that many CTTS are found in the same location as the WTTS in this diagram, even though CTTS photometric variability is probably due to a mixture of hot and cold surface spots (see Paper I). This is not unexpected, however : as long as the surface spots never disappear from view as the star rotates, the system's mean light level as well as its extrema will be driven by spot modulation, regardless of the spot's temperature. Hence, the system will have no preferred brightness state ($C2 \simeq 0.5$) and its extreme values will exhibit about the same amount of variability ($C1 \simeq 1$). More extreme values of the $C1$ and $C2$ parameters are expected only in the particular case of a low latitude hot spot located at the surface of a highly inclined system, in which case the spot disappears for part of the rotational cycle.

That CTTS share the same location as WTTS in this diagram thus does not imply that their source of variability is the same. It does imply, however, that surface spots in most CTTS, as in most WTTS, never disappear from view as the system rotates. In turn, this suggests that hot accretion spots in CTTS are located at relatively high latitudes on the stellar surface, as expected from accretion from the inner disk edge onto a slightly tilted dipolar

magnetosphere. In addition, the impact of hot spots on photometric variations is expected to be more conspicuous at shorter wavelengths (e.g., U and B-bands) than at V (Bouvier & Bertout 1989).

7. Conclusions

Our main conclusion is that most WTTS have very stable long term variability with relatively small changes of amplitude or mean light level. The long term variability seen merely reflects modulation in the cold spot distributions. Photometric periods are stable over many years, as is the phase of minimum light for most objects, within some range. On the long term, the spot properties do change in subtle ways, leading to some variations in the shape and amplitudes of the light curves. The long term variability of WTTS is thus perhaps best understood by assuming that they are covered by a number of spots unevenly distributed on the stellar surface and located at preferential longitudes and/or latitudes, much like active belts in the Sun and RS CVn systems, rather than resulting from a single polar spot. Such an uneven spot distribution would account for the reported correlation between amplitude and brightness level, as well as for the quasi-sinusoidal shape of the light curves, which indicates that the unspotted photosphere is not seen in these stars at any rotational phase. It also implies that the coverage of the stellar photosphere by cold spots may be much larger than anticipated from simple modelling of the light curves, which only provide lower limits to the spot areal coverage. Doppler imaging of a sample of typical WTTS could be an effective means to obtain further constraints on the distribution of cold spots at the surface of WTTS.

Modelling of the light curves for V819 Tau, V827 Tau, V830 Tau and V836 Tau indicates that the spotted regions cover as much as 30 to 90% of the visible stellar hemisphere and that the mean temperature of the spots is 500–1400 K lower than the ambient photosphere. More detailed model calculations of the light curve of V410 Tau showed that:

(i) The decrease in mean brightness is attributable to the increase in total spot area from 47 to 53% and that it is essentially independent of the degree of nonuniformity in the spot distribution over the surface.

(ii) The amplitude of the phased light curve depends on the degree of nonuniformity in the spot distribution more strongly than on the stars total spot area. An increase in amplitude was accompanied by an increase in the degree of nonuniformity in the spot distribution over the stellar surface from 21 to 35%.

(iii) There is a weak correlation between the star's total spot area and its degree of nonuniformity in the spot distribution with the correlation coefficient $k=0.71$. The increase in the stars total spot area from 47 to 53% was accompanied by a decrease in the degree of nonuniformity in the spot distribution from 35 to 21%.

The most active variable stars in our sample (i.e. those with the largest amplitudes) demonstrate stabil-

ity of phase of minimum light most strongly over many years. The data presented here should prove useful in further investigations of the nature and evolution of spots on WTTS.

Acknowledgements. The authors wish to thank O. Ezhkova, M. Ibrahimov, V. Kondratiev, S. Yakubov, S. Artemenko and many other observers and students, who worked or are still working in the Tashkent Astronomical Institute, for their participation in the photometric observations. We are particularly grateful to C. Dougados, C. Bertout, and F. M enard for their comments and suggestions pertaining to this work. Support of the American Astronomical Society, European Southern Observatory (grant A-02-048), and International Science Foundation by Soros (grant MZA000) and a CRDF grant (ZP1-341) is acknowledged. This work was also supported by a NATO Collaborative Linkage grant for European countries (PST.CLG.976194) and by an ECO-NET program of the French Ministry of Foreign Affairs, which we both gratefully acknowledge. W.H. gratefully acknowledges the support of NASA through its Origins of Solar Systems Program. We especially thank the referee F. Vrba for helpful comments on the original version of this manuscript.

8. References

- Alekseev, I. Y. & Gershberg, R. E. 1996a, AZh, 73, 589
 Alekseev, I. Y. & Gershberg, R. E. 1996b, AZh, 73, 579
 Attridge, J. M. & Herbst, W. 1992, *Astrophys.J. (Lett.)*, 398, L61
 Berdnikov, L. N., Grankin, K. N., Chernyshev, A. V., et al. 1991, *Soviet Astron. Lett.*, 117, 23
 Bouvier, J. & Bertout, C. 1989, *A&A*, 211, 99
 Bouvier, J., Bertout, C., Benz, W., et al. 1986, *A&A*, 165, 110
 Bouvier, J., Boutelier, T., Alencar, S., et al. 2005, in *Protostars and Planets V* (LPI Contribution No. 1286.), 8150
 Bouvier, J., Cabrit, S., Fernandez, M., et al. 1993, *A&A*, 272, 176
 Bouvier, J., Covino, E., Kovo, O., et al. 1995, *A&A*, 299, 89
 Bouvier, J., Forestini, M., & Allain, S. 1997a, *A&A*, 326, 1023
 Bouvier, J., Wichmann, R., Grankin, K., et al. 1997b, *A&A*, 318, 495
 Butler, C. J. 1996, *Proc. IAU Symposium*, 176, 423
 Choi, P. I. & Herbst, W. 1996, *Astron.J.*, 111, 283
 Cohen, R., Herbst, W., & Williams, E. 2004, *Astron.J.*, 127, 1602
 Covino, E., Terranegra, L., Franchini, M., et al. 1992, *A&AS*, 94, 273
 Eaton, N. L., Herbst, W., & Hillenbrand, L. 1995, *Astron.J.*, 110, 1735
 Edwards, S. E., Strom, S., & Hartigan, P. H. 1993, *Astron.J.*, 106, 372
 Ehgamberdiev, S. A., Bajjumanov, A. K., Ilyasov, S. P., et al. 2000, *A&AS*, 145, 293
 Ghez, A. M., Neugebauer, G., & Matthews, K. 1993, *AJ*, 106, 2005

- Grankin, K., Melnikov, S., Bouvier, J., et al. 2007, *A&A*, 461, 183
- Grankin, K. N. 1991, *Inform. Bull. Var. Stars.*, N3658
- Grankin, K. N. 1992, *Inform. Bull. Var. Stars.*, N3720
- Grankin, K. N. 1993, *Inform. Bull. Var. Stars.*, N3823
- Grankin, K. N. 1994, *Inform. Bull. Var. Stars.*, N4042
- Grankin, K. N. 1996, *Inform. Bull. Var. Stars.*, N4316
- Grankin, K. N. 1997, *Astron. Lett.*, 23, 700
- Grankin, K. N. 1997, in *Low Mass Star Formation - from Infall to Outflow.*, ed. F. Malbet & A. Castets (Proc. IAU Symposium N. 182. Dordrecht: D. Reidel Publ. Company.), 281
- Grankin, K. N. 1998, *Astron. Lett.*, 24, 580
- Grankin, K. N. 1999, *Astron. Lett.*, 25, 611
- Grankin, K. N., Granzer, T., & Strassmeier, K. 2002, in *1st Potsdam Thinkshop Poster Proceedings.* (Potsdam, Germany, May 6-10), 77
- Grankin, K. N., Ibragimov, M. A., Kondratiev, V. B., et al. 1995, *AZh*, 72, 894
- Herbig, G. H. & Bell, K. R. 1988, *Lick Obs. Bull.*, 1111, 1
- Herbst, W. 1989, *Astron.J.*, 98, 2268
- Herbst, W., Herbst, D. K., Grossman, E. J., et al. 1994, *AJ*, 108, 1906
- Herbst, W. & Mundt, R. 2005, *ApJ*, 633, 967
- Horne, J. H. & Baliunas, S. L. 1986, *AJ*, 302, 757
- Horne, K., Wade, R. A., & Szkody, P. 1986, *MNRAS*, 219, 791
- Irwin, J., et al. 2007, *MNRAS*, 380, 541
- Joncour, I., Bertout, C., & Bouvier, J. 1994a, *A&A*, 291, L19
- Joncour, I., Bertout, C., & Menard, F. 1994b, *A&A*, 285, L25
- Landolt, A. U. 1983, *AJ*, 88, 439
- Landolt, A. U. 1992, *AJ*, 104, 340
- Leinert, C., Zinnecker, H., Weitzel, N., et al. 1993, *A&A*, 278, 129
- Losh, H. M. 1939, *Pub. Zurich Obs*, 2
- Mandel, G. N. & Herbst, W. 1991, *Astrophys.J. (Lett.)*, 383, L75
- Mathieu, R. D., Walter, F. M., & Myers, P. C. 1989, *AJ*, 98, 987
- Mundt, R., Walter, F. M., Feigelson, E. D., et al. 1983, *ApJ*, 269, 229
- Nemec, A. F. L. & Nemec, J. M. 1985, *AJ*, 90, 2317
- Nikonov, V. 1976, *Izvestiya KrAO*, 54, 3
- Petrov, P., Shcherbakov, V., Berdyugina S. et al. 1994, *Astron. Astrophys. Suppl. Ser.*, 107, 9
- Press, W. H. & Rybicki, G. B. 1989, *ApJ*, 338, 277
- Reipurth, B. & Zinnecker, H. 1993, *A&A*, 278, 81
- Rice, J. & Strassmeier, K. 1996, *A&A*, 316, 164
- Rydgren, A. E. & Vrba, F. J. 1983, *ApJ*, 267, 191
- Rydgren, A. E., Zak, D. S., Vrba, F. J., et al. 1984, *AJ*, 89, 1015
- Shevchenko, V. S. 1989, *Herbig Ae/Be Stars* (in Russian) (Tashkent: FAN)
- Shevchenko, V. S., Ezhkova, O. V., Kondratiev, V. B., et al. 1995, *Inform. Bull. Var. Stars.*, N4206
- Shevchenko, V. S. & Herbst, W. 1998, *AJ*, 116, 1419
- Shu, F., Najita, J., Ruden, S., et al. 1994, *ApJ*, 429, 797
- Stelzer, B., Fernandez, M., Costa, V. M., et al. 2003, *A&A*, 411, 517
- Strauzis, V. 1977, *Multicolor Stellar Photometry* (Vilnius: Mokslas)
- Vogt, S. S. 1981, *ApJ*, 250, 327
- Vrba, F. J., Chugainov, P. F., Weaver, W. B., et al. 1993, *AJ*, 106, 1608
- Vrba, F. J., Herbst, W., & Booth, J. 1988, *Astron.J.*, 96, 1032
- Walter, F. M., Brown, A., Linsky, J. L., et al. 1987, *ApJ*, 314, 297
- White, R. J. & Ghez, A. M. 2001, *ApJ*, 556, 265
- Zakirov, M. M., Azimov, A. A., & Grankin, K. N. 1993, *Inform. Bull. Var. Stars.*, N3898

Table 1. Results of Maidanak long-term photometry of WTTS

Name	HBC	SpT	JD _{min} -JD _{max}	N _s	V range	N _{obs}	$\overline{B-V}$	$\overline{V-R}$	Multiplicity	Ref.
Anon 1	366	M0	48953-50760	6	13.58-13.36	96	1.84	1.84		
HD 283572	380	G6 IV	48854-53300	13	9.16-8.89	425	0.77	0.70		
Hubble 4	374	K7	49197-49251	1	12.71-12.59	27	1.62			
LkCa 1	365	M4	49213-50760	5	13.80-13.64	88	1.45	1.71		
LkCa 2		K7	48953-51157	7	12.37-12.19	119	1.39	1.34		
LkCa 3	368	M1	48858-51157	7	12.17-11.97	144	1.48	1.52	VB (0."48)	wh01
LkCa 4	370	K7	48858-53289	13	13.19-12.28	284	1.42	1.37		
LkCa 5	371	M2	48953-50081	4	13.63-13.44	65	1.47	1.50		
LkCa 7	379	K7	48182-53300	15	12.75-12.11	422	1.36	1.35	VB (1."02)	wh01
LkCa 11		M2	48954-53291	13	13.33-13.10	197	1.50	1.58		
LkCa 14	417	M0	48954-50081	4	11.84-11.63	63	1.19	1.05		
LkCa 16	420	K7	48859-53289	4	12.71-12.32	61	1.50	1.41	VB (0."29)	wh01
LkCa 19	426	K0	48181-53300	13	11.08-10.80	308	1.01	1.09		
LkCa 21	382	M3	48952-49251	2	13.54-13.34	32	1.57	1.65		
SR 9	264	K5	46607-52827	15	11.86-11.28	336	1.25	1.21	VB (0."59)	gh93
SR 12	263	M1	46964-52819	10	13.53-13.09	195	1.57	1.60		
TAP 4	347	K1	48858-49218	2	12.26-12.01	33	0.88	0.80		
TAP 9	351	K5	48858-49635	3	12.25-12.08	82	1.05	0.99	VB (0."61)	le93
TAP 10AB	352+353	G0+G5	48953-49623	3	11.42-11.29	56	0.87	0.80	VB (8."6)	he88
TAP 11AB	354+355	K3+K0	48853-49218	2	12.50-12.36	31	0.92	0.83		
TAP 14NE	356+357	K2	48853-49215	2	12.96-12.86	28	1.01	0.89		
TAP 26	376	K7	48858-50760	6	12.44-12.16	165	1.13	1.01		
TAP 35	388	K1	48860-53300	8	10.45-10.16	226	0.77	0.67		
TAP 40	392	K5	48860-50760	6	12.69-12.52	137	1.17	1.05		
TAP 41	397	K7	48860-53300	13	12.41-12.01	245	1.24	1.11		
TAP 45	403	K7	48860-53291	8	13.36-13.11	145	1.45	1.33		
TAP 49	407	G8	48860-50020	4	12.82-12.58	86	1.03	0.91		
TAP 50	408	K0 IV	49199-53311	12	10.34-10.06	263	0.89	0.79		
TAP 57NW	427	K7	48857-53300	13	11.74-11.47	276	1.28	1.16	SB (P \approx 2000d)	ma89
V501 Aur		K2	49659-53311	10	10.83-10.54	247	1.62	1.35		
V410 Tau	29	K3	46660-53300	19	11.24-10.52	959	1.16	1.04	VT (0."07, 0."29)	wh01
V819 Tau	378	K7	48126-53272	15	13.30-12.77	363	1.51	1.46	VB (10."5)	le93
V826 Tau	400	K7	48135-49625	4	12.19-12.04	94	1.38	1.27	SB (P=3.9d)	mu83
V827 Tau	399	K7	48136-53299	14	13.00-12.24	236	1.42	1.37		
V830 Tau	405	K7	48127-53298	15	12.39-11.91	383	1.35	1.24		
V836 Tau	429	K7	48143-53292	11	14.05-13.01	170	1.53	1.44		
V1197 Tau		G8	49659-53300	10	10.66-10.49	232	0.84	0.75		
V1199 Tau		K0	49659-53311	10	10.75-10.53	208	0.72	0.66		
V1200 Tau		G5	49659-53311	10	11.35-11.15	212	0.93	0.81		
V1202 Tau		G0	49659-53311	10	10.95-10.68	208	0.83	0.71		
V1207 Tau		K7	49659-53300	10	12.01-11.81	174	1.24	1.08		
VY Tau	68	M0	46383-52176	17	13.98-13.25	436	1.47	1.47	VB (0."66)	wh01
Wa CrA/1	676	K0 IV	48049-48100	1	11.67-11.35	27	1.17	1.08		
Wa CrA/2	678	G8 IV	48049-48100	1	10.69-10.53	28	0.85	0.74		
Wa Oph/1	630	K2 IV	49145-53228	8	12.19-11.84	190	1.38	1.30		
Wa Oph/2	633	K1 IV	51733-53228	5	11.77-11.60	101	1.16	1.11		
Wa Oph/3	634	K0 IV	49145-53228	9	10.98-10.73	255	1.19	1.07		
Wa Oph/4	652	K4	49147-52059	4	13.72-10.44	104	1.88	1.83	VB (8."7)	re93

Table 1. References

wh01: White & Ghez (2001); re93: Reipurth & Zinnecker (1993); mu83: Mundt et al. (1983); ma89: Mathieu et al. (1989); le93: Leinert et al. (1993); he88: Herbig & Bell (1988); gh93: Ghez et al. (1993).

Table 2. The results of periodogram analysis.

Name	1986	1987	1988	1989	1990	1991	1992	1993	1994	1995	1996	1997	1998	1999	2000	2001	2002	2003	2004	all data
Anon 1								6.38	6.44	6.45	-	-								6.493
HD 283572							1.531	1.533	1.549	1.544	1.546	1.539		1.526	1.547	1.539	1.537	1.427?	1.533	1.546
LkCa 1								2.502?	2.494:	-	2.505:	-								2.513:
LkCa 2								-	-	1.363	1.166?	1.368								1.367
LkCa 3							7.30	-	7.43	7.34	7.52	7.12								7.35
LkCa 4							3.376	3.367	3.373	3.376	3.376	3.373	3.381	3.373	3.376	3.376	3.376	3.376	3.387	3.376
LkCa 7					5.70	5.66	5.67	5.67	5.65	5.67	5.66	5.65	5.67	5.70	5.61	5.67	5.67	5.64	5.64	5.666
LkCa 11								1.542	1.541?	1.540	1.543	-	-	1.539						1.5396
LkCa 19					2.245	2.233	2.233	2.235?	-	2.237			2.227	2.240	2.237		2.240	2.238	2.238	2.228?
SR 9	6.36	6.59	6.54	-	6.54	6.68:		6.53	6.53		6.56		6.29:				6.34			6.55
SR 12			-	3.407:	3.497	3.578		3.506	3.410											3.515
TAP 4							0.482													0.482
TAP 26							0.714	0.714	0.714?	0.833	-	0.717								0.7134?
TAP 35							2.78	2.74	2.75	-	-	2.88					2.75	-	-	-
TAP 40							1.553	1.552	-	-	-	-								1.555
TAP 41							2.424	2.421	2.417	2.421	2.427	2.417	2.421	2.424				2.418	2.429	2.427
TAP 45							-	9.73	-	-	9.98?	9.98:						9.76:		9.90
TAP 49							3.30?	3.14?	-	-	-	-								-
TAP 50							3.04	3.01	-	3.05	3.04		3.02		-	-	-	-	3.03	3.017?
TAP 57NW							9.35	9.46	-	9.37	9.22?	9.37	9.15:	-		9.11	9.32:	9.71	9.11	-
V501 Aur								43	56	56	52	52	-						61	55.6
V410 Tau	1.871	1.873	1.873	1.872	1.873	1.872	1.872	1.872	1.872	1.872	1.872	1.874	1.874	1.872	1.877	1.872	1.872	1.872	1.874	1.8718
V819 Tau					5.58	5.61	5.54	5.50	5.51	5.51	5.51	5.51	5.53	5.49	5.52	5.51:	5.48	5.73	5.533:	-
V827 Tau					3.76	3.77	3.75	3.76	3.76	-	3.76	3.76	3.77	3.70					3.77	3.759
V830 Tau					2.738	2.744	2.738	2.740	2.740	2.742	2.740	2.738	2.745	2.740	2.745:	2.677?	-	-		2.742
V836 Tau					6.75	6.68?	6.77		6.75	6.77	6.76	6.80								6.757
V1197 Tau								2.67	-	-	2.65	2.64	2.66		-	-	-	-	2.67	2.628
V1199 Tau								1.818	-	-	1.824	-	1.815		-	1.840?	1.804:	1.827?	1.810:	-
V1200 Tau								1.599	1.592	-	1.605	1.592	-		-	-	-	-	1.606	1.596
V1202 Tau								2.712	2.663:	-	2.686	2.685	2.740						2.681	2.695
V1207 Tau								7.74	7.80	-	7.53:	-	7.53			7.72		7.75	8.10	-
VY Tau		5.39	5.38	5.35	-	-	-	5.30		5.35	5.48:	5.44	-	-	-					5.369
Wa CrA/1					2.25															2.25
Wa CrA/2					2.80															2.80
Wa Oph/1								3.82	3.81					3.78	3.82	3.80	3.77	3.78?	3.71:	-
Wa Oph/3								1.523	1.517		1.526				1.527	1.455	1.501	-	1.518	1.527

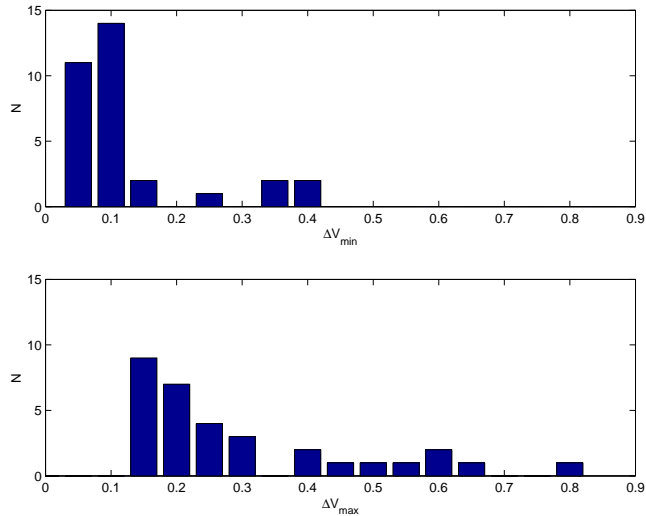


Fig.1. Distribution of minimum and maximum amplitudes among WTTS.

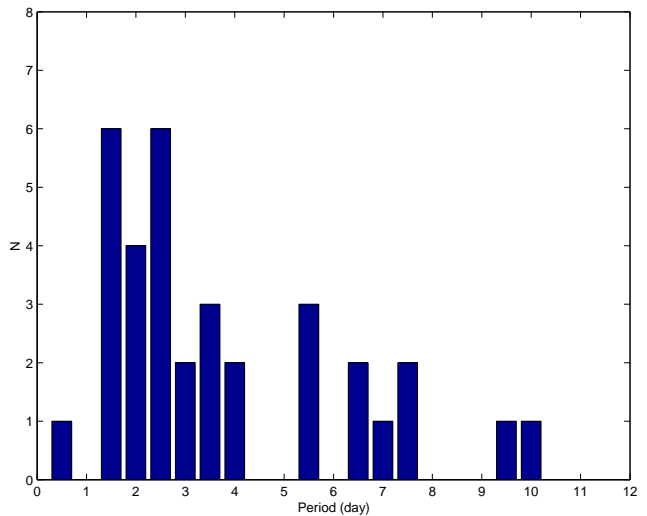


Fig.2. Stellar rotation period distribution for 36 WTTS with well-determined periods.

Table 3. WTTS with well-known periods.

Name	Epoch of observ.	ΔV_{min} (mag)	ΔV_{max} (mag)	Initial Epoch JDH 2400000+	Period (day)	References (1)	References (2)
Anon 1	1992-1997	0.11	0.20	48951.7	6.493	gr96	gr97
HD 283572	1992-2004	0.08	0.24	48850.3	1.529	wa87	gr97
LkCa 1	1993-1997	0.06	0.14	49212.8	2.497	gr96	gr97
LkCa 2	1992-1998	0.05	0.18	49950.3	1.3614	gr96	this paper
LkCa 3	1992-1998	0.08	0.16	48856.5	7.35	gr96	this paper
LkCa 4	1992-2004	0.35	0.79	46296.8	3.374	gr93	this paper
LkCa 7	1990-2004	0.33	0.58	45998.9	5.6638	gr92	gr97
LkCa 11	1993-2004	0.12	0.19	48952.0	1.5396	gr96	this paper
LkCa 19	1990-2004	0.09	0.15	48179.8	2.236	gr93	gr97
SR 9	1986-2003	0.24	0.55	46607.0	6.531	bo89	this paper
SR 12	1987-2003	0.15	0.41	46963.5	3.516	bo89	this paper
TAP 4	1992-1993	0.08	0.22	48853.3	0.482	this paper	this paper
TAP 26	1992-1997	0.08	0.27	48619.6	0.7135	gr93	gr97
TAP 35	1992-2004	0.05	0.13	48858.5	2.734	gr93	gr97
TAP 40	1992-1997	0.09	0.13	48859.8	1.5548	gr93	gr97
TAP 41	1992-2004	0.11	0.39	48857.9	2.425	gr93	this paper
TAP 45	1992-2004	0.09	0.21	48859.5	9.909	gr94	gr97
TAP 49	1992-1995	0.07	0.12	48857.2	3.32	gr94	gr97
TAP 50	1993-2004	0.05	0.13	49195.3	3.039	gr94	this paper
TAP 57NW	1992-2004	0.10	0.21	48848.7	9.345	za93	gr97
V501 Aur (W185)	1994-2004	0.05	0.24	49625.7	55.95	bo97	this paper
V410 Tau	1986-2004	0.39	0.63	46659.6	1.87197	ry83	st03
V819 Tau	1990-2004	0.12	0.28	48122.4	5.53113	ry84	this paper
V827 Tau	1990-2004	0.07	0.51	48136.3	3.75837	bo86	this paper
V830 Tau	1990-2004	0.15	0.45	48124.7	2.74101	ry84	this paper
V836 Tau	1990-2004	0.39	0.62	48142.9	6.75791	ry84	this paper
V1197 Tau (W123)	1994-2004	0.06	0.16	49658.0	2.662	bo97	this paper
V1199 Tau (W130)	1994-2004	0.06	0.21	49658.0	1.8122	bo97	this paper
V1200 Tau (W139)	1994-2004	0.08	0.13	49659.3	1.605	bo97	this paper
V1202 Tau (W145)	1994-2004	0.06	0.19	49658.8	2.7136	bo97	this paper
V1207 Tau (W188)	1994-2004	0.06	0.14	49656.9	7.741	bo97	this paper
VY Tau	1985-2001	0.11	0.31	44610.7	5.36995	gr91	gr94
Wa CrA/1	1990	0.32	0.32	48048.3	2.24	sh95	sh95
Wa CrA/2	1990	0.16	0.16	48048.3	2.79	co92	sh95
Wa Oph/1	1993-2004	0.10	0.30	48986.1	3.792	za93	this paper
Wa Oph/3	1993-2004	0.06	0.23	49144.3	1.5214	sh98	this paper

Table 3. References

be91: Berdnikov et al. (1991); bo86: Bouvier et al. (1986); bo89: Bouvier & Bertout (1989); bo97: Bouvier et al. (1997b); co92: Covino et al. (1992); gr91: Grankin (1991); gr92: Grankin (1992); gr93: Grankin (1993); gr94: Grankin (1994); gr96: Grankin (1996); gr97: Grankin (1997); ry83: Rydgren & Vrba (1983); ry84: Rydgren et al. (1984); sh95: Shevchenko et al. (1995); sh98: Shevchenko & Herbst (1998); st03: Stelzer et al. (2003); wa87: Walter et al. (1987); za93: Zakirov et al. (1993).

Table 4. Statistical properties of WTTS light curves (see text).

Name	N_s^*	\overline{V}_m	σ_{V_m}	$\overline{\Delta V}$	$\sigma_{\Delta V}$	$\frac{\sigma_{\Delta V}}{\overline{\Delta V}}$	$\frac{\Delta(B-V)}{\overline{\Delta V}}$	ρ_{B-V}	$\frac{\Delta(V-R)}{\overline{\Delta V}}$	ρ_{V-R}	c1	c2
Anon 1	5	13.445	0.015	0.156	0.036	0.230	0.142	0.13	0.376	0.60	0.503	0.175
HD 283572	12	9.000	0.028	0.133	0.045	0.342	0.245	0.44	0.246	0.56	0.486	0.551
LkCa 1	5	13.710	0.007	0.097	0.033	0.343	-0.363	-0.22	0.709	0.72	0.407	0.841
LkCa 2	5	12.286	0.016	0.096	0.053	0.549	-0.001	0.00	0.338	0.68	0.592	1.034
LkCa 3	6	12.034	0.017	0.118	0.029	0.245	-0.041	-0.07	0.290	0.59	0.341	0.437
LkCa 4	13	12.624	0.078	0.512	0.122	0.238	0.035	0.22	0.188	0.79	0.489	0.432
LkCa 7	15	12.423	0.025	0.438	0.078	0.178	0.112	0.39	0.228	0.81	0.481	0.924
LkCa 11	10	13.213	0.022	0.154	0.025	0.164	0.004	0.01	0.302	0.48	0.457	1.249
LkCa 19	12	10.915	0.041	0.117	0.023	0.200	0.092	0.19	0.309	0.69	0.540	0.848
SR 9	12	11.524	0.048	0.417	0.099	0.239	0.152	0.37	0.208	0.75	0.377	0.796
SR 12	6	13.288	0.026	0.303	0.087	0.288	0.226	0.25	0.218	0.44	0.495	0.254
TAP 26	6	12.320	0.044	0.164	0.064	0.390	0.045	0.12	0.368	0.72	0.559	1.380
TAP 35	8	10.276	0.063	0.089	0.031	0.351	0.087	0.32	0.082	0.26	0.477	0.822
TAP 40	6	12.608	0.022	0.109	0.018	0.160	-0.145	-0.19	0.286	0.47	0.484	1.474
TAP 41	12	12.181	0.025	0.236	0.090	0.380	0.082	0.24	0.170	0.53	0.543	0.666
TAP 45	8	13.205	0.031	0.131	0.038	0.292	-0.086	-0.11	0.259	0.47	0.473	0.770
TAP 50	10	10.197	0.044	0.088	0.027	0.309	0.320	0.61	0.324	0.67	0.488	0.994
TAP 57NW	13	11.620	0.025	0.153	0.044	0.290	0.162	0.23	0.359	0.59	0.514	0.961
V501 Aur	9	10.637	0.044	0.142	0.070	0.492	0.120	0.29	0.124	0.31	0.387	0.255
V410 Tau	19	10.863	0.044	0.534	0.073	0.137	0.113	0.58	0.154	0.79	0.406	0.978
V819 Tau	14	13.050	0.113	0.197	0.046	0.231	0.105	0.35	0.203	0.73	0.550	1.103
V827 Tau	12	12.528	0.105	0.252	0.127	0.505	0.140	0.48	0.234	0.82	0.475	0.684
V830 Tau	14	12.183	0.043	0.253	0.081	0.319	0.103	0.30	0.207	0.68	0.416	2.776
V836 Tau	8	13.382	0.196	0.500	0.084	0.168	0.020	0.07	0.201	0.86	0.422	0.973
V1197 Tau	10	10.564	0.019	0.095	0.030	0.312	0.203	0.25	0.290	0.37	0.477	0.821
V1199 Tau	10	10.643	0.031	0.099	0.046	0.464	0.041	0.08	0.218	0.50	0.476	1.044
V1200 Tau	9	11.247	0.028	0.098	0.017	0.179	0.137	0.22	0.299	0.50	0.552	0.893
V1202 Tau	10	10.811	0.036	0.112	0.035	0.313	0.204	0.40	0.292	0.58	0.472	0.887
V1207 Tau	9	11.920	0.026	0.092	0.028	0.308	0.062	0.09	0.250	0.46	0.501	1.057
VY Tau	15	13.650	0.080	0.218	0.091	0.419	0.286	0.30	0.356	0.70	0.542	1.445
Wa Oph/1	7	12.007	0.065	0.165	0.072	0.436	-0.083	-0.14	0.338	0.68	0.457	1.015
Wa Oph/2	5	11.676	0.025	0.114	0.032	0.285	0.276	0.34	0.196	0.36	0.445	0.672
Wa Oph/3	8	10.835	0.023	0.149	0.054	0.362	0.200	0.30	0.210	0.45	0.484	0.542

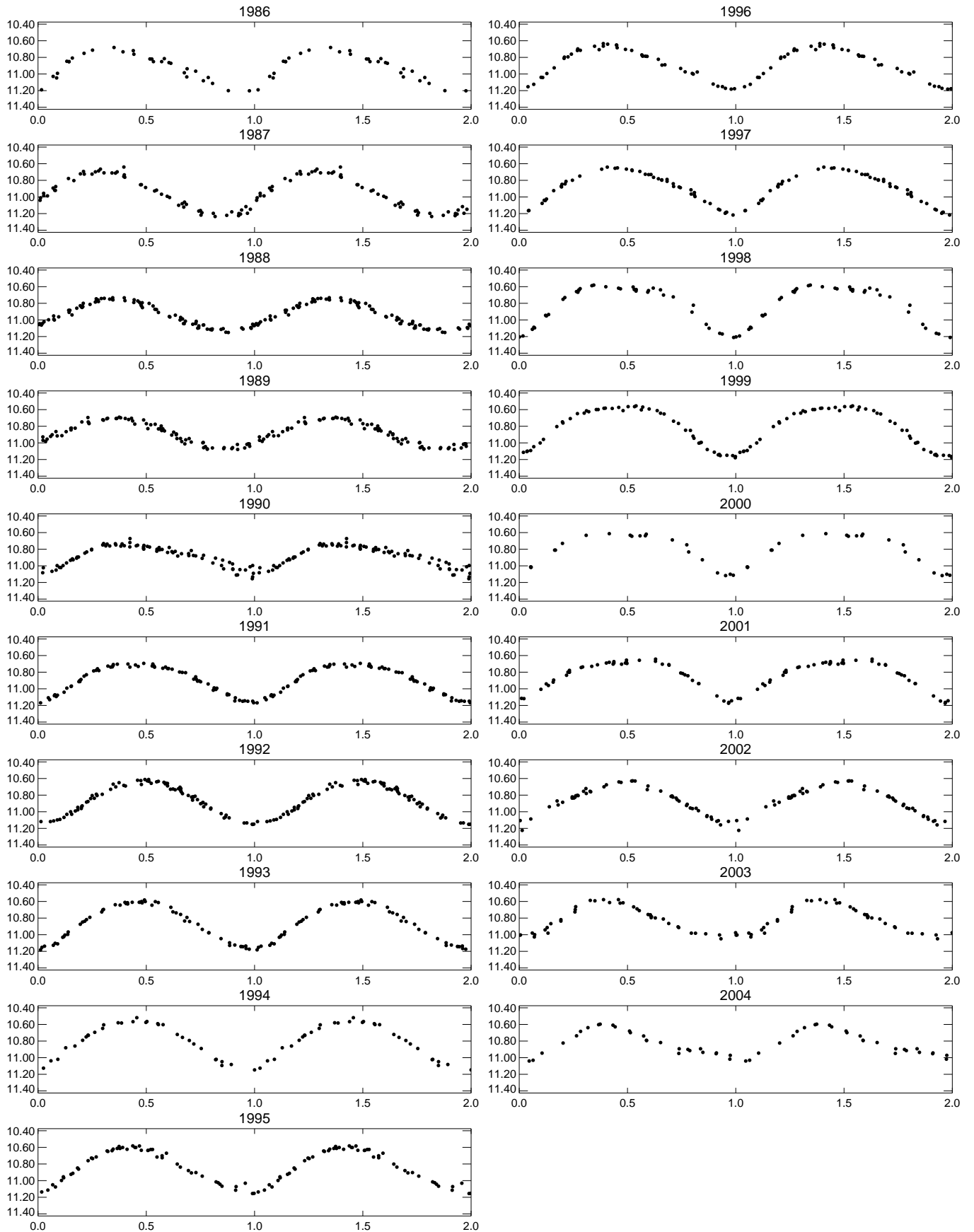


Fig.3. Phased light curves of V410 Tau for each season. The phased light curve conserves the phase of light minimum (ϕ_{min}) over several years.

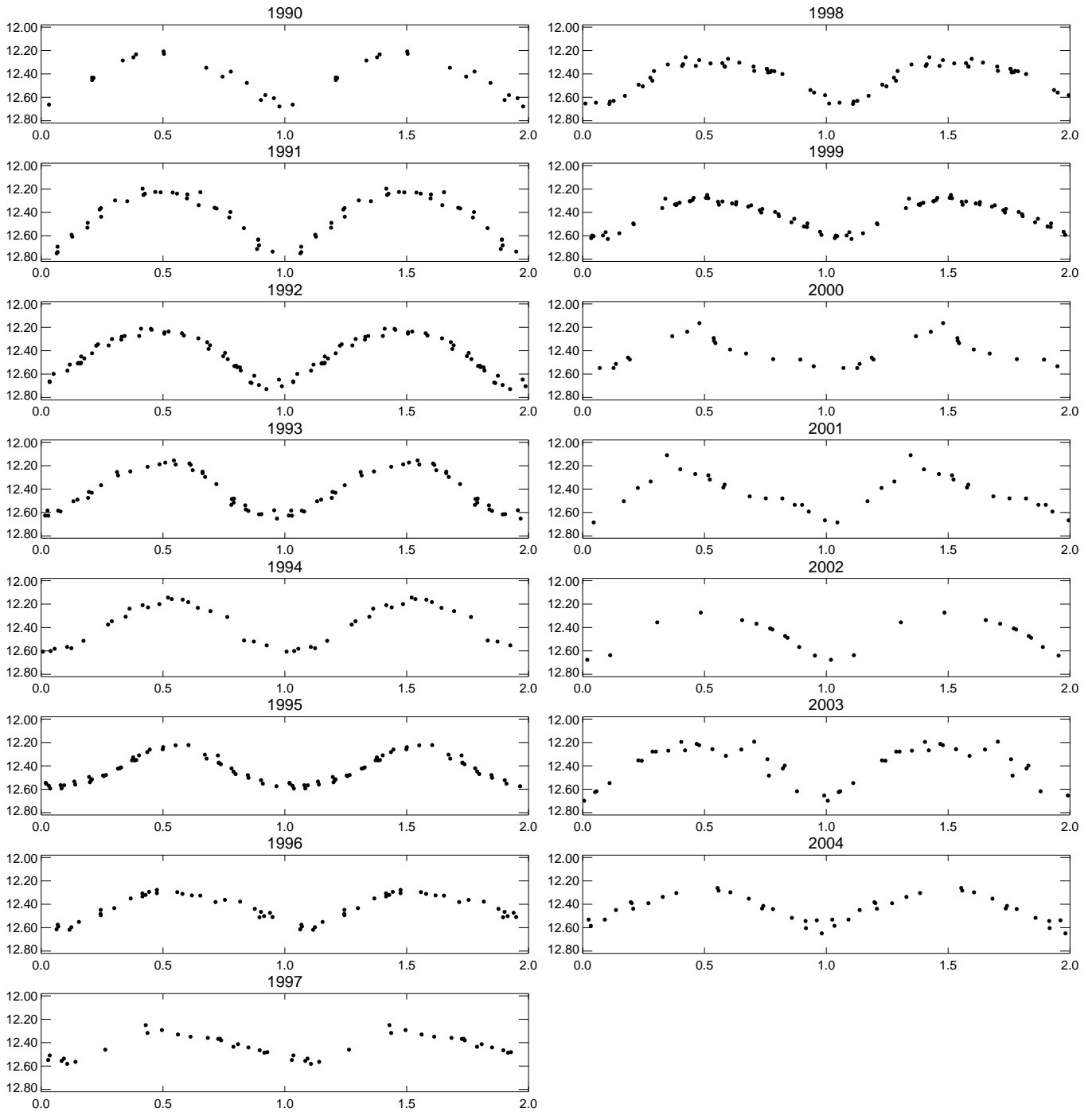


Fig.4. Phased light curves of LkCa 7. This is another example of the phenomenon of ϕ_{min} stability. At the same time it is possible to see some changes of amplitude and shape of a light curve.

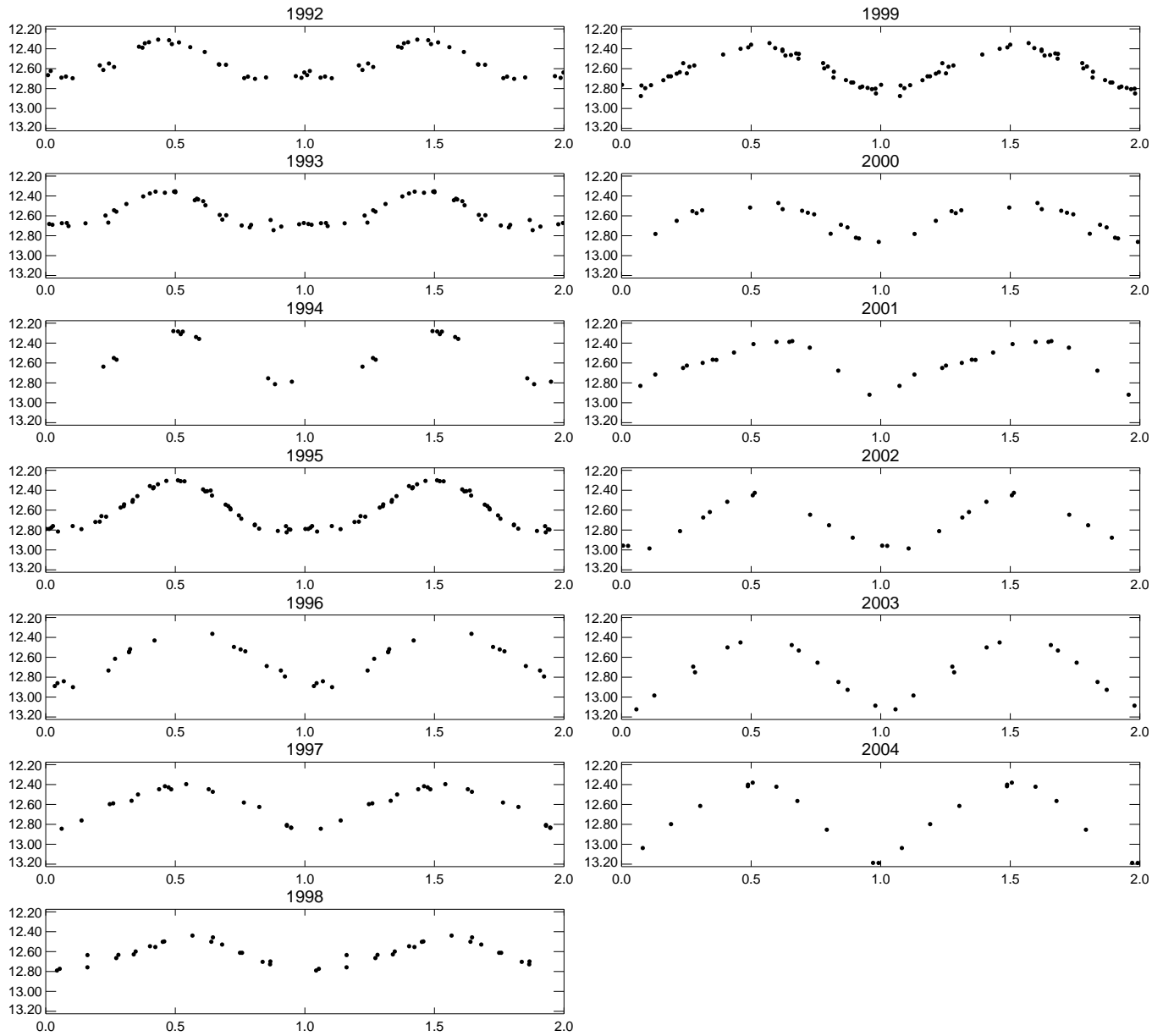


Fig.5. Phased light curves of LkCa 4. This star shows the highest amplitude of periodic light variation in our sample (0.79^m).

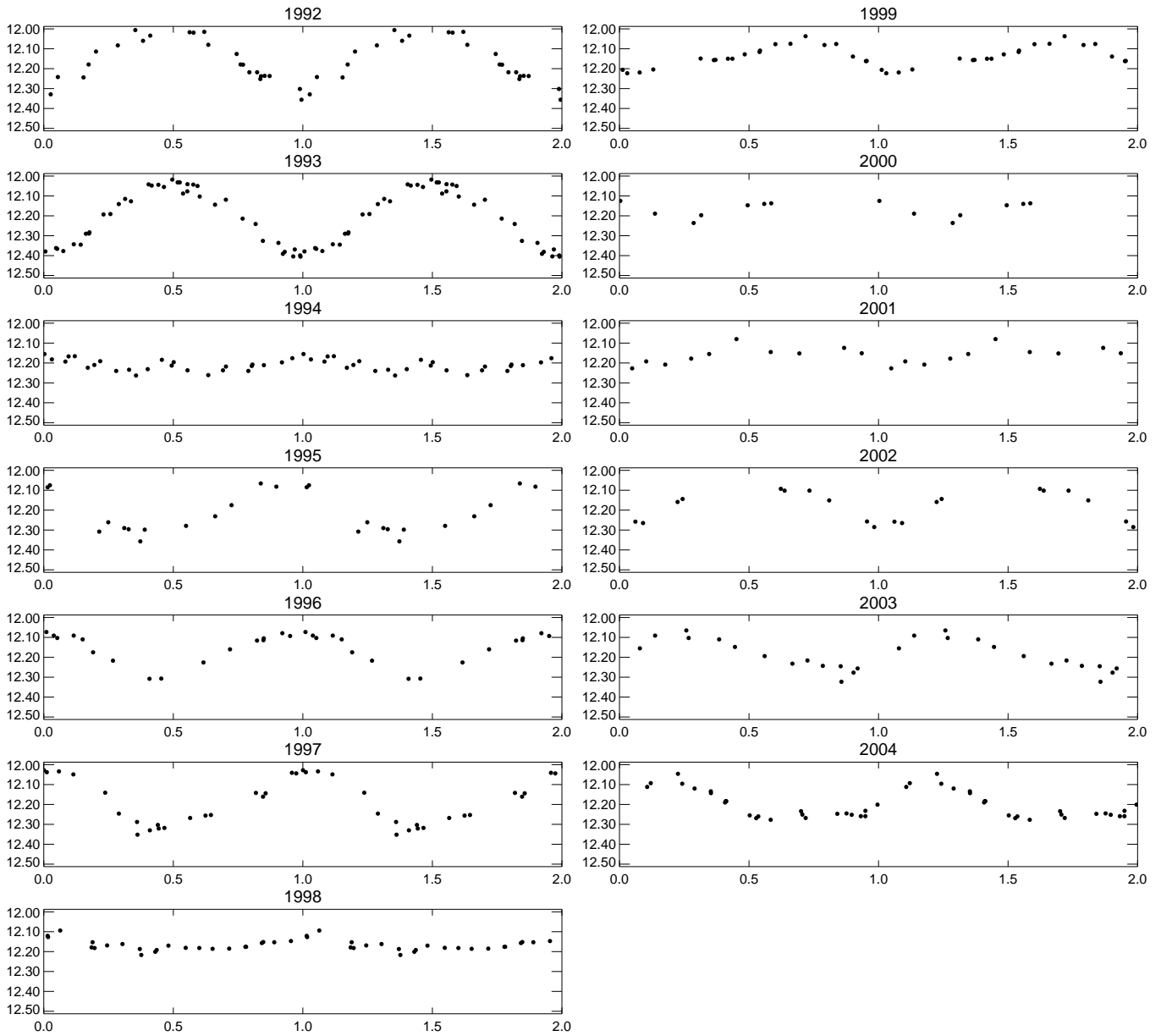


Fig.6. Phased light curves of TAP 41. The amplitude of the periodic light variations changes appreciably (by a few tenths of a magnitude) from season to season.

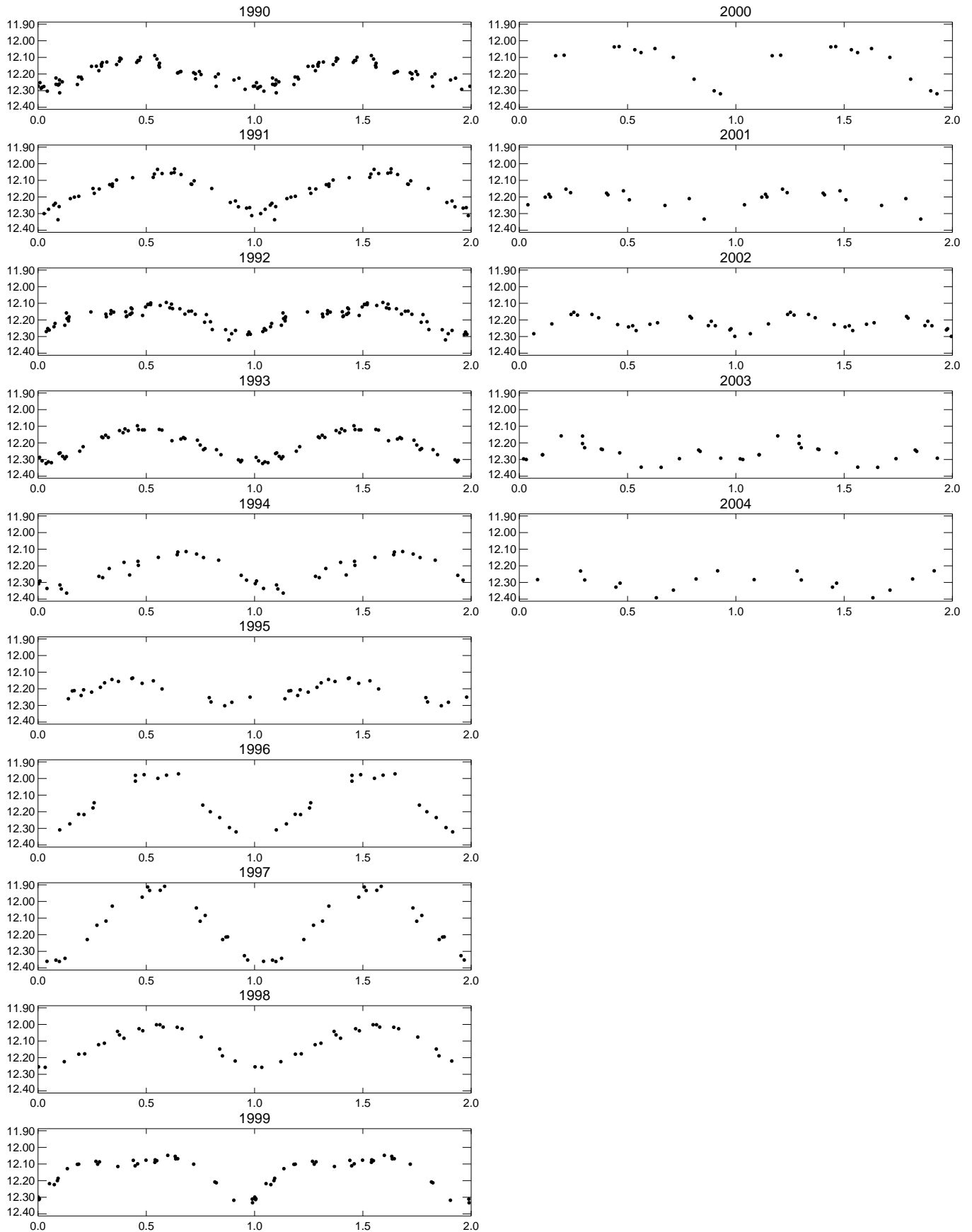


Fig.7. Phased light curves of V830 Tau. During 2002-2003 the phased light curve had a complicated shape consisting of two maxima and two minima during each cycle.

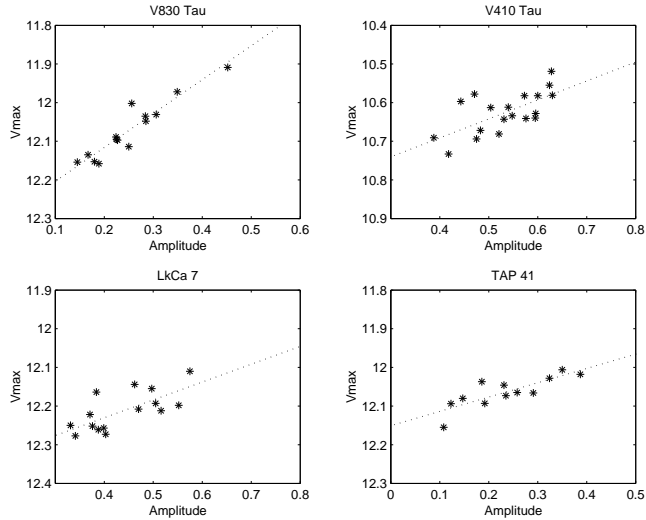


Fig.8. Illustrations of the linear relation found for some WTTS between the level of maximum brightness in a season and the amplitude of the variability during the same season.

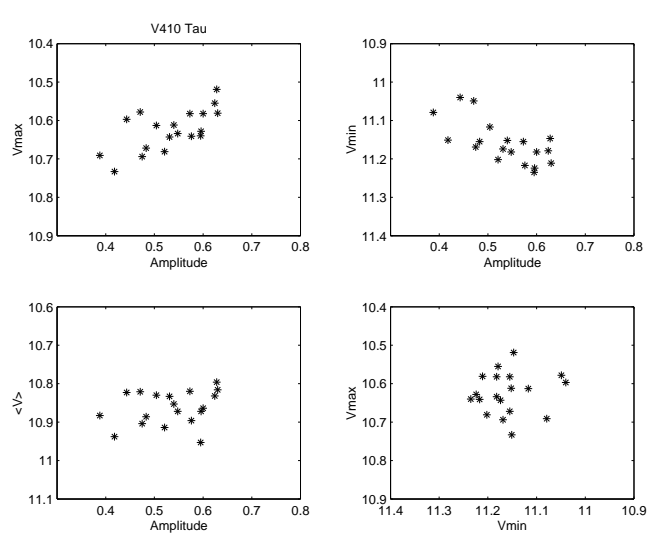


Fig.9. Dependencies between amplitude, average level of light, Vmin and Vmax for V410 Tau in different seasons.

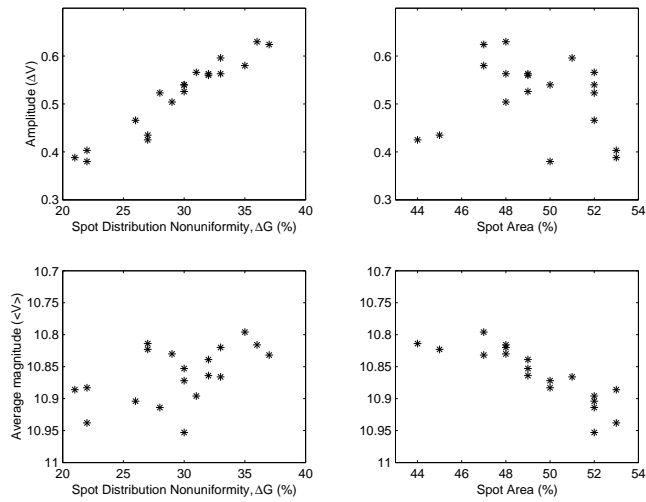


Fig.10. Plots of the amplitude (top) and the average level of brightness (bottom) of V410 Tau against the non-uniformity in the spot distribution (left) and the total spot area (right).

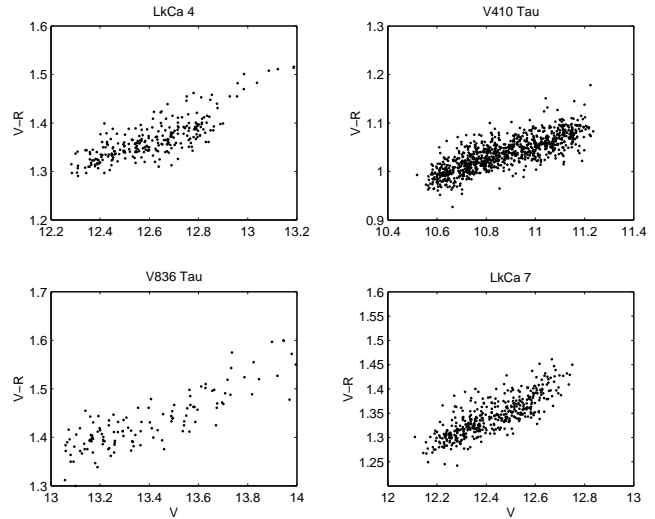


Fig.11. Illustrations of the linear relations found for most objects between $V - R$ colour and V magnitude. Colour slopes and correlation factors are listed in Table 4.

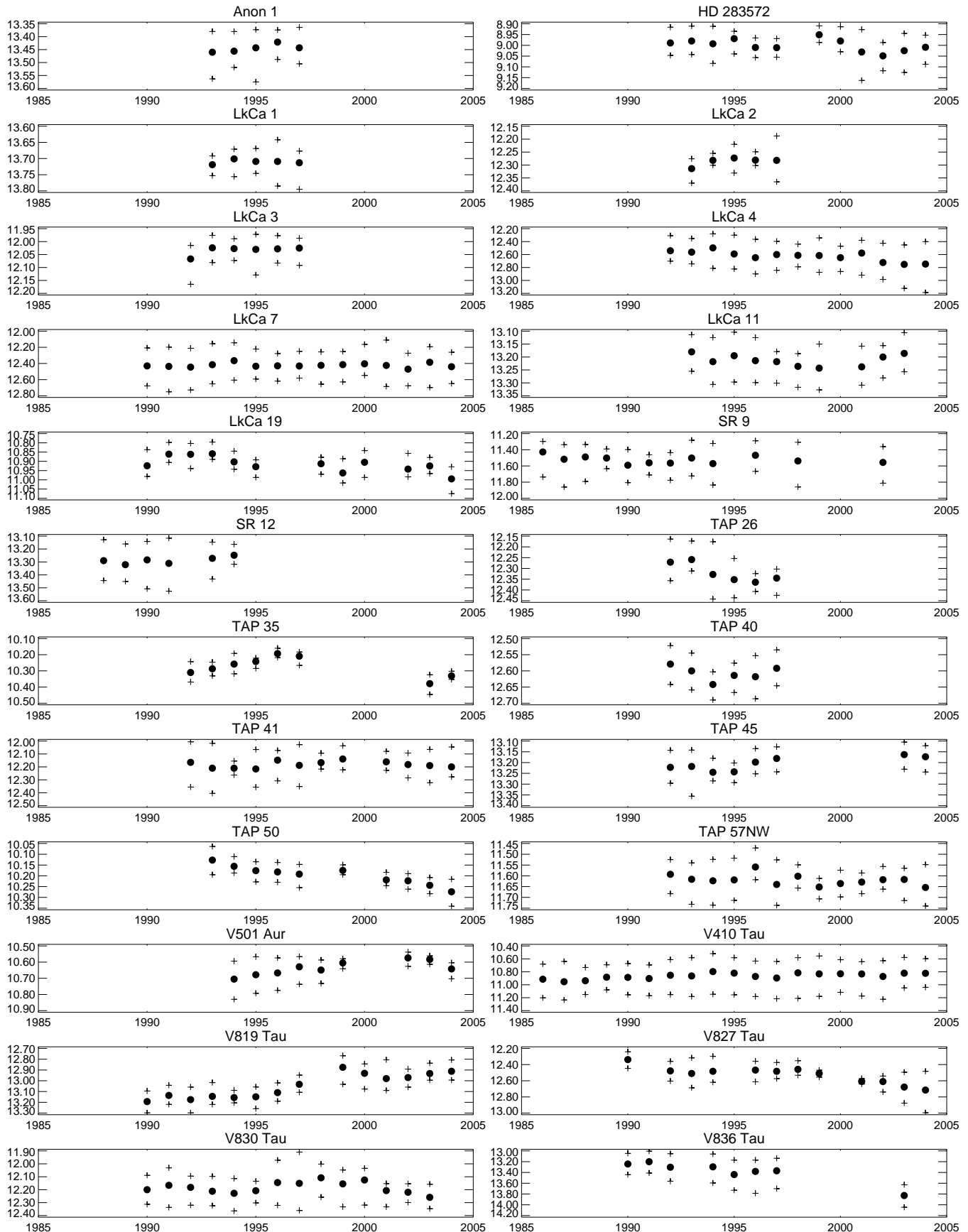


Fig.12a. Long term V-band light curves of 33 WTTS observed at Mt. Maidanak. The mean brightness level is shown by a filled circle for each observing season and the minimum and maximum brightness values by crosses.

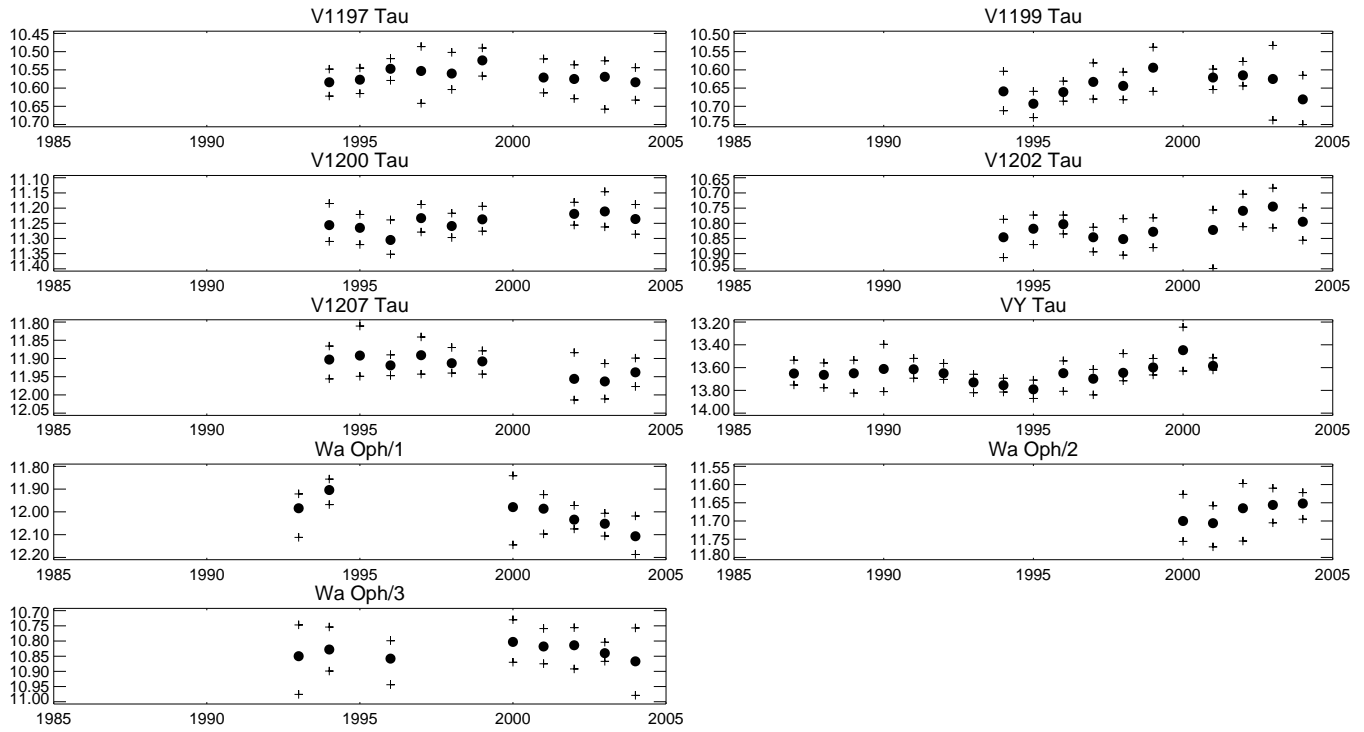


Fig.12b. (Continue of Fig. 12a.)

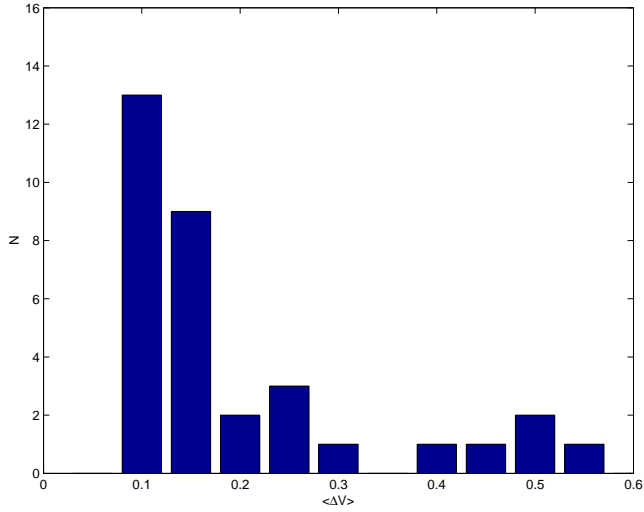


Fig.13. Average photometric amplitude in the V-band for the 33 WTTS of our sample ($\langle \Delta V \rangle$).

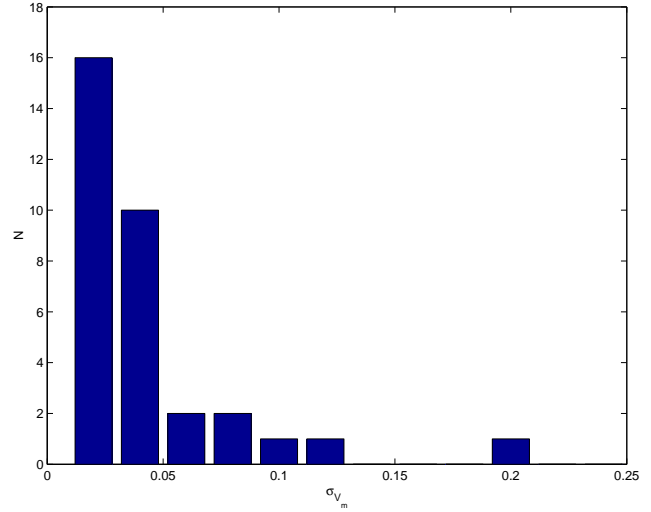


Fig.14. Standard deviation of the seasonal mean brightness level (σ_{V_m}).

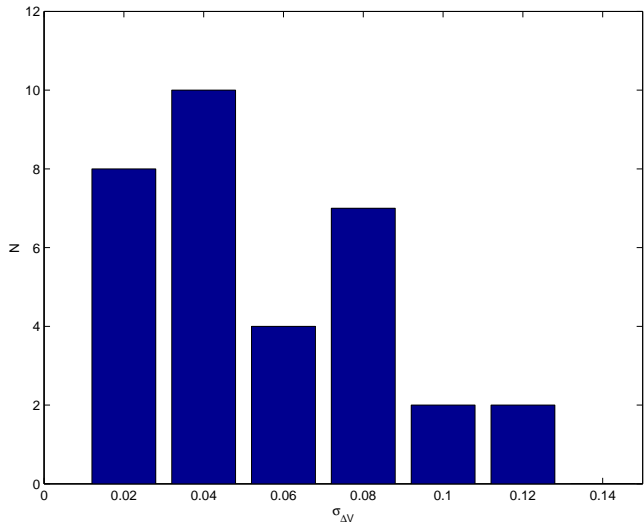


Fig.15. Standard deviation of the seasonal photometric amplitude ($\sigma_{\Delta V}$).

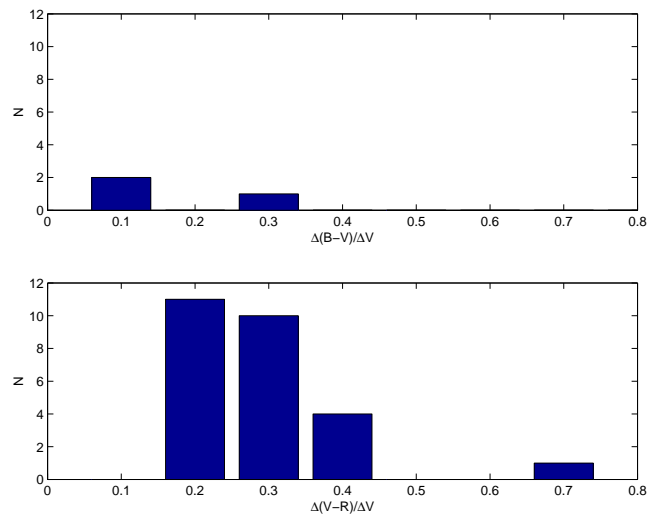


Fig.16. Least-square color slopes. Top panel : $\frac{\Delta(B-V)}{\Delta V}$; lower panel: $\frac{\Delta(V-R)}{\Delta V}$.

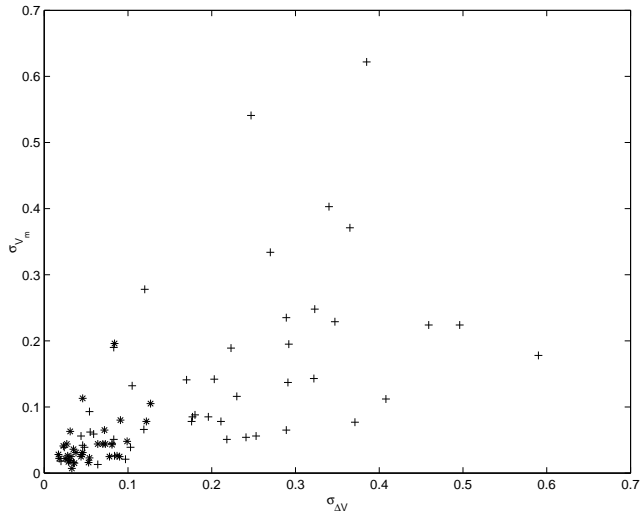


Fig.17. Variability of the mean brightness level versus the variability of the photometric amplitude. 33 WTT stars are denoted by asterisks and 49 CTTs are denoted by crosses.

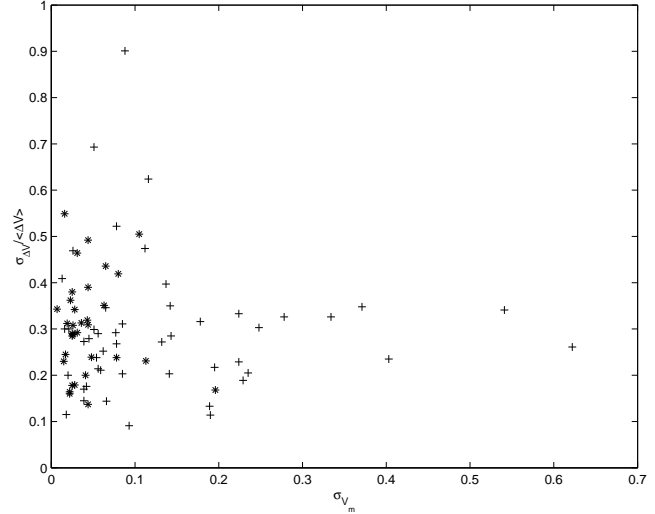


Fig.18. The relative variation of amplitude versus the variation of the mean brightness level.

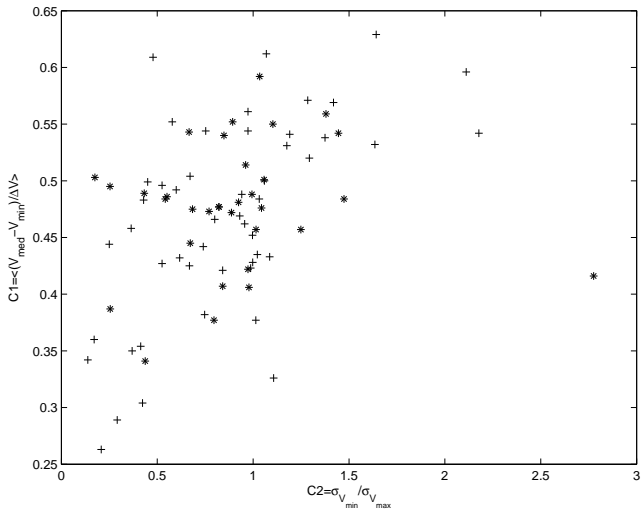


Fig.19. The star's preferred brightness state (as measured by $C1 = \langle \frac{V_{med} - V_{min}}{\Delta V} \rangle$) is plotted against the relative variations of its extreme brightness states (as measured by $C2 = \sigma_{V_{min}} / \sigma_{V_{max}}$). See text.